

NASA/TP–2018-219033/Vol. 3



Advances in Above- and In-Water Radiometry, Volume 3:

Hybridspectral Next-Generation Optical Instruments

*Stanford B. Hooker, Randall N. Lind, John H. Morrow, James W. Brown, Raphael M. Kudela,
Henry F. Houskeeper, and Koji Suzuki*

National Aeronautics and
Space Administration

Goddard Space Flight Center
Greenbelt, Maryland 20771

November 2018

NASA STI Program ... in Profile

Since its founding, NASA has been dedicated to the advancement of aeronautics and space science. The NASA scientific and technical information (STI) program plays a key part in helping NASA maintain this important role.

The NASA STI program operates under the auspices of the Agency Chief Information Officer. It collects, organizes, provides for archiving, and disseminates NASA's STI. The NASA STI program provides access to the NASA Aeronautics and Space Database and its public interface, the NASA Technical Report Server, thus providing one of the largest collections of aeronautical and space science STI in the world. Results are published in both non-NASA channels and by NASA in the NASA STI Report Series, which includes the following report types:

- **TECHNICAL PUBLICATION.** Reports of completed research or a major significant phase of research that present the results of NASA Programs and include extensive data or theoretical analysis. Includes compilations of significant scientific and technical data and information deemed to be of continuing reference value. NASA counterpart of peer-reviewed formal professional papers but has less stringent limitations on manuscript length and extent of graphic presentations.
- **TECHNICAL MEMORANDUM.** Scientific and technical findings that are preliminary or of specialized interest, e.g., quick release reports, working papers, and bibliographies that contain minimal annotation. Does not contain extensive analysis.
- **CONTRACTOR REPORT.** Scientific and technical findings by NASA-sponsored contractors and grantees.
- **CONFERENCE PUBLICATION.** Collected papers from scientific and technical conferences, symposia, seminars, or other meetings sponsored or co-sponsored by NASA.
- **SPECIAL PUBLICATION.** Scientific, technical, or historical information from NASA programs, projects, and missions, often concerned with subjects having substantial public interest.
- **TECHNICAL TRANSLATION.** English-language translations of foreign scientific and technical material pertinent to NASA's mission.

Specialized services also include organizing and publishing research results, distributing specialized research announcements and feeds, providing help desk and personal search support, and enabling data exchange services. For more information about the NASA STI program, see the following:

- Access the NASA STI program home page at <http://www.sti.nasa.gov>
 - E-mail your question via the Internet to help@sti.nasa.gov
 - Phone the NASA STI Information Desk at 757-864-9658
 - Write to:
NASA STI Information Desk
Mail Stop 148
NASA's Langley Research Center
Hampton, VA 23681-2199
-



Advances in Above- and In-Water Radiometry, Volume 3:

Hybridspectral Next-Generation Optical Instruments

Stanford B. Hooker
NASA Goddard Space Flight Center Greenbelt, Maryland

Randall N. Lind
Biospherical Instruments Inc. San Diego, California

John H. Morrow
Biospherical Instruments Inc. San Diego, California

James W. Brown
RSMAS University of Miami Miami, Florida

Raphael M. Kudela
University of California Santa Cruz Santa Cruz, California

Henry F. Houskeeper
University of California Santa Cruz Santa Cruz, California

Koji Suzuki
Hokkaido University Sapporo, Japan

National Aeronautics and
Space Administration

Goddard Space Flight Center
Greenbelt, Maryland 20771

Notice for Copyrighted Information

This manuscript has been authored by employees of *Biospherical Instruments Inc.*, *RSMAS University of Miami*, *Hokkaido University*, and *University of California Santa Cruz* with the National Aeronautics and Space Administration. The United States Government has a non-exclusive, irrevocable, worldwide license to prepare derivative works, publish, or reproduce this manuscript, and allow others to do so, for United States Government purposes. Any publisher accepting this manuscript for publication acknowledges that the United States Government retains such a license in any published form of this manuscript. All other rights are retained by the copyright owner.

Trade names and trademarks are used in this report for identification only. Their usage does not constitute an official endorsement, either expressed or implied, by the National Aeronautics and Space Administration.

Level of Review: This material has been technically reviewed by technical management.

Available from

NASA STI Program
Mail Stop 148
NASA's Langley Research Center
Hampton, VA 23681-2199

National Technical Information Service
5285 Port Royal Road
Springfield, VA 22161
703-605-6000

ABSTRACT

This publication documents the scientific advances associated with new instrument systems and accessories built to improve above- and in-water observations of the apparent optical properties (AOPs) for a diversity of water masses, including optically complex waters. The principal objective is to be prepared for the launch of next-generation ocean color satellites with the most capable commercial off-the-shelf (COTS) instrumentation in the shortest time possible. The technologies described herein are entirely new hybrid sampling capabilities, so as to satisfy the requirements established for next-generation missions. Both above- and in-water instruments are documented with software options for autonomous control of data collection activities as applicable. The instruments were developed for the Hybridspectral Alternative for Remote Profiling of Optical Observations for NASA Satellites (HARPOONS) vicarious calibration project. The state-of-the-art accuracy required for vicarious calibration also led to the development of laboratory instruments to ensure the field observations were within uncertainty requirements. Separate detailed presentations of the individual instruments provide the hardware designs, accompanying software for data acquisition and processing, and examples of the results achieved.

Prologue

The HARPOONS optical instruments are from the Compact-Profiling Hybrid Instrumentation for Radiometry and Ecology (C-PHIRE) class of next-generation radiometers, wherein an array of microradiometers (15 or 18, depending on the instrument) acquire data in parallel with a hyperspectral spectrograph (2,048 pixels). In order to reduce costs, a common architecture is used for all of the above- and in-water optical instruments derived from a harmonized design approach with differences minimized to the greatest extent practicable. Depending on the instrument type, C-PHIRE radiometers span the ultraviolet (UV), visible (VIS), near-infrared (NIR), and short-wave infrared (SWIR) domains.

The HARPOONS project requires an autonomous deployment capability for making vicarious calibration observations in the open ocean during clear-sky and fair-weather conditions over a 10 d mission time period (Chap. 8). Liquid Robotics Inc. (LRI) manufactures (Sunnyvale, California) a second-generation Wave Glider surface vessel, denoted an SV2, plus a third-generation (SV3) model with greater payload and power specifications. The latter is used, because the former does not meet the power requirements for the profiling system configured with the new C-PHIRE radiometers (Chap. 7).

The deployment of sophisticated instruments designed to provide the highest quality data products possible requires advances in the technologies used in the laboratory and the field. Consequently, the HARPOONS activity involves five principal instrument systems, as follows:

1. A Towable Optical Wave-Following *In Situ* Hybrid (TOW-FISH) profiler measures the downward irradiance (E_d) and upwelling radiance (L_u) using in-water radiometers mounted on a backplane with two digital thrusters. The backplane is towed behind

an SV3 using a sea cable with terminated internal and external strength members. The thrusters are used to ascend the backplane from a resting depth to the surface, whereupon the backplane sinks back to the resting depth. C-PHIRE light observations are recorded for both the up and down casts, and low-level thrust can be used to further stabilize the planar orientation of the radiometers.

2. An above-water suite of instruments mounted on the SV3, which is comprised principally of a global solar irradiance (E_s) C-PHIRE radiometer equipped with a shadow band accessory to measure the indirect or diffuse irradiance (E_i), collects data simultaneously with the in-water instruments. The other above-water data that are recorded provide the photosynthetically available radiation (PAR) and global positioning system (GPS) coordinates. A set of antennas provide WiFi, cellular, and satellite (Iridium) communications. The diffusers for the solar reference and PAR sensor are higher than any of the other above-water systems, so these data are always unperturbed.
3. An above-water Compact-Optical Sensors for Planetary Radiant Energy (C-OSPReY) sun photometer mounted on a tracker with a quad detector, which is supported by a solar reference (E_s and E_i) similar to what is mounted on the SV3, measures the direct solar (or lunar) irradiance (E), the indirect or diffuse sky radiance (L_i), and the total radiance of the sea surface (L_T), location permitting. The wavelength domain for this C-PHIRE instrument suite is more expansive (UV–SWIR) than the SV3 instrument suite (UV–NIR).
4. A laboratory C-PHIRE Transfer Radiometer (CXR) in a radiance (L) embodiment and designated the

CXL maintains the National Institute of Standards and Technology (NIST) scale of spectral irradiance within a Lamp Library of NIST-traceable standard lamps and seasoned working lamps. Transferring the NIST scale to a working lamp increases the lifetime of the standard lamps by minimizing the amount of time the standard lamps are used.

5. A Compact Quality Monitor (CQM) provides a time series of the calibration stability of radiometers. The CQM can be used in the laboratory or the field, and is anticipated to be a routine part of laboratory calibrations.

The control of the individual instruments or systems and the recording of the data obtained are accomplished using the Data Acquisition and Control for Photometric and Radiometric Observations (DACPRO) software environment. Both manual and automated modes are available. DACPRO is strongly linked to the Processing of

Radiometric Observations of Seawater using Information Technologies (PROSIT) software package, which is used to derive all of the data products from the field and laboratory observations across all wavelengths. An overall description of the two software environments is presented in Sect. 8.3.3 and more detailed information for DACPRO and PROSIT are provided in Sects. 8.7.1 and 8.7.2, respectively.

The DACPRO and PROSIT software systems are accessible using more than one operating system (OS), but they are both optimized for Macintosh OS X. Although DACPRO is usually hosted on a MacBook Pro laptop, a MacMini was used for the SV3 because of the smaller form factor and low power requirements. An international user group evaluates DACPRO and PROSIT functionality during recurring field campaigns, workshops, and training sessions, which result in recommendations to improve the software by identifying problems and desirable new features.

Chapter 9

The C-PHIRE Instruments

STANFORD B. HOOKER
NASA Goddard Space Flight Center
Greenbelt, Maryland

RANDALL N. LIND AND JOHN H. MORROW
Biospherical Instruments, Inc.
San Diego, California

JAMES W. BROWN
RSMAS University of Miami
Miami, Florida

ABSTRACT

The hybridspectral C-PHIRE radiometer design is based on a harmonized approach to simplify component inventories and lower costs. C-PHIRE radiometers have two separate detector systems incorporating an array of 15 or 18 silicon photodetector (SiP) microradiometers plus a 2,048 pixel Compact Grating Spectrometer (CGS). The former has 10 decades of dynamic range with a limited number of wavelengths, whereas the latter has limited dynamic range and high resolution spectral coverage. The two complementary detector systems can be intracompared during data processing to verify stability and detect anomalous performance and drift. The CGS uses a universal serial bus (USB) for data telemetry. Consequently, additional electronics are necessary to overcome USB distance limitations as required for in-water profiling and for siting a solar reference to ensure an unobstructed view of the sky. For SWIR wavelengths, e.g., for sun photometry (C-OSPReY), indium gallium arsenide (InGaAs) photodiodes are used.

9.1 Introduction

An Expandable Technologies for Radiometric Applications (XTRA) instrument is a fixed wavelength radiometer with an array of SiP microradiometers (usually 19). Instrument suites built with XTRA radiometers include the Compact-Optical Profiling System (C-OPS), as well as the Coastal Airborne Instrument Radiometers (C-AIR) and the more advanced the Compact-Airborne Environmental Radiometers for Oceanography (C-AERO). The former is principally an in-water profiling system, with an above-water solar references, whereas the latter two are both exclusively above-water systems. The three-letter codes distinguishing the radiometers involved are as follows:

- XAL XTRA above-water radiance,
- XAE XTRA above-water irradiance,
- XPE XTRA profiler (in-water) irradiance, and
- XPL XTRA profiler (in-water) radiance.

The XAE global solar irradiance radiometer is used with all three instrument suites.

An Enhanced Performance Instrument Class (EPIC) instrument is a hybridspectral radiometer, i.e., it has two

detector technologies that function contemporaneously in the same housing while viewing the same target. Prior EPIC radiometers include the above-water Optical Sensors for Planetary Radiant Energy (OSPReY) sun photometer and solar reference (Hooker et al. 2012), with the reference the most similar to the C-PHIRE design. The two EPIC detector technologies are an array of fixed wavelength SiP microradiometers (typically 15–18, depending on the radiometer model) and a hyperspectral spectrograph (256 or 2,048 pixels, depending on the heritage). C-PHIRE radiometers incorporate a 2,048 pixel spectrograph identical to the one used with the C-HyR accessory, whereas OSPReY radiometers use a 256 pixel spectrograph.

Unlike legacy radiometers, which were built primarily for narrowly specified light sources and sampling targets, EPIC instrument suites were anticipated to view a multitude of sources and targets under varying conditions. Consequently, the EPIC instrument embodiment was designated as either EPIC Multitarget Radiometer (EMR) radiance (L) or irradiance (E), i.e., EML or EME, respectively. Only the OSPReY instrumentation suite was built with this architecture, which included two OSPReY

transfer radiometer (OXR) designs with radiance and irradiance embodiments, i.e., OXL and OXE, respectively.

The C-PHIRE hybridspectral instrument combines the positive aspects of both of the XTRA and EPIC technologies into a next-generation EPIC design for field and laboratory measurements. Presently, the only laboratory instrument is the CXL, although an irradiance version is anticipated. For brevity and specificity, an individual radiance and irradiance field radiometer is distinguished by whether it was designed to make observations above water or to make a profile of observations in water. This distinction translates to a three-letter code patterned after the aforementioned XTRA designators:

- EAL EPIC above-water radiance,
- EAE EPIC above-water irradiance,
- EPE EPIC profiler (in-water) irradiance, and
- EPL EPIC profiler (in-water) radiance.

The EAE global solar irradiance radiometer is used with all three instrument suites.

The most complex instrument is a C-PHIRE EAL sun photometer (C-OSPRey), which is fitted with a nine-position filter wheel. The filter wheel rotates one of two neutral density (ND) filters in front of the spectrograph fiber for bright targets (e.g., the Sun) and has three-axis polarization filters (0° , 45° , and 90°) plus a 395 nm cut-on filter for improved stray light characterization.

For most deployment configurations, the C-PHIRE radiometers are located rather far away from the data acquisition computer, e.g., the TOW-FISH uses a sea cable that can be 100 m in length. Because the data telemetry for C-PHIRE radiometers is based on the USB interface, distances between the instruments and the acquisition computer must nominally be 2–3 m or less. Consequently, for longer distances as required for TOW-FISH profiling, additional electronics are necessary to overcome the distance limitations of USB.

The EPIC Remote Interface (ERI) provides power conditioning and the communications channel conversion for USB to support EPIC class radiometers when they are located more than 2–3 m from the data acquisition computer. There are two versions of the ERI, as follows: a) above-water atmospheric, which is designated ERA; and, b) in-water profiling, which is designated, ERP. The C-OSPRey solar irradiance reference, and the C-OSPRey radiance radiometer (i.e., sun photometer) use identical ERA modules.

In an installation embodiment such as the SV3, the C-PHIRE solar irradiance reference does not require an ERA because of its proximity to the data acquisition computer (i.e., less than 2–3 m). It is also possible certain deployment scenarios of C-OSPRey could be envisioned, wherein an ERA for the solar irradiance reference would not be necessary. For example, if the data acquisition computer was in a structure, the solar reference could be on the roof and perhaps within 2–3 m of the computer.

The ERI is located with the radiometric instrument system where it is mounted. To convert back to USB at the end of a long cable at the data acquisition computer, another set of electronics are needed. This conversion allows the acquisition commands to be transmitted to the instrument and the received data recorded. The conversion back to USB takes place in a Hybridspectral Power (HyPower) box (Sect. 3.3.3) or one of its variants, e.g., a HyPower2 box, which is a more capable version that has two cable ports rather than one. Like the ERI, there are two versions of the HyPower2 box; the most advanced version is designated the HyPower2+ box and it is intended to be used with C-OSPRey.

9.2 Background

The design of C-PHIRE instruments is based on the successful production of two prior hybridspectral instruments: the above-water OSPRey sun photometer with solar reference and the in-water C-HyR accessory. The OSPRey radiance and irradiance instruments differ in aspects of their designs (e.g., they have a different number of microradiometers), which increased the complexity in manufacturing them. Consequently, the C-PHIRE radiometers use a harmonized design to the greatest extent practicable to simplify component inventories and lower costs. With respect to OSPRey radiometers, C-PHIRE instruments are smaller in size to make them more compact, which also lowers the weight and facilitates deployment options, e.g., the TOW-FISH.

The size reduction of a C-PHIRE radiometer, with respect to the otherwise rather similar OSPRey instruments, is achieved by removing or incorporating design elements with respect to prior XTRA and EPIC instrument suites (Hooker et al. 2012), as follows:

1. The spectrograph is the same CGS model (2,048 pixels) used with the C-HyR accessory (Chap. 3) and is from the same manufacturer, Carl Zeiss Spectroscopy GmbH (Jena, Germany), of the OSPRey spectrograph (256 pixels);
2. The spectrograph fiber is fed through the microradiometer array by removing one microradiometer, which is the same approach used for the OSPRey solar reference (Hooker et al. 2012);
3. The filter wheel used with the C-PHIRE sun photometer, (i.e., C-OSPRey), is the same one used for the OSPRey sun photometer, except the C-OSPRey filter wheel is incorporated by removing an additional three microradiometers, thereby resulting in 15 microradiometers for C-OSPRey, and it uses an encoder for more accurate positioning; and
4. The OSPRey active heating system for radiometers is omitted, primarily because the primary first application of C-PHIRE radiometers on the in-water TOW-FISH, which operates from batteries, is incompatible with active heating.

Table 18. The instrument systems influencing the C-PHIRE and C-OSPRey designs, wherein the radiometer types, the principal measured light parameters, the number of fixed wavelength (FWL) microradiometer channels plus the number of hyperspectral spectrograph (HSG) pixels (if applicable), and the physical specifications are given. The latter includes the outer diameter (OD), length, and weight. Measurements of E_i are obtained with the Biospherical Shadow band Accessory for Diffuse Irradiance (BioSHADE) accessory, which is not used in airborne instrument suites (i.e., C-AIR and C-AERO). The above-water radiance instruments capable of sun viewing (i.e., C-AIR, C-AERO, OSPRey, and C-OSPRey) can be equipped with removal or permanently affixed shrouds, as indicated.

Instrument System			Detectors		OD		Length		Weight	
Name	Type	Parameters	FWL	HSG	[in]	[cm]	[in]	[cm]	[lb]	[kg]
C-OPS	XAE	E_s and E_i	19		2.75	7.0	13.3	33.8	3.3	1.5
C-OPS	XPE	E_d	19		2.75	7.0	13.3	33.8	3.3	1.5
C-OPS	XPL	L_u	19		2.75	7.0	10.0	25.4	2.8	1.3
C-AIR	XAE	E_s	19		2.75	7.0	13.3	33.8	3.3	1.5
C-AIR	XAL	E , L_i , and L_T	19		2.75	7.0	14.7	37.3	3.6	1.6
C-AERO	XAE	E_s	19		2.75	7.0	13.3	33.8	3.3	1.5
C-AERO¶	XAL	E , L_i , and L_T	19		2.75	7.0	18.7	47.5	4.1	1.9
OSPRey	EME	E_s and E_i	18	256	6.00	15.2	19.7	50.0	14.2	6.4
OSPRey	EML	E , L_i , and L_T	19	256	6.00	15.2	22.9	58.2	15.4	7.0
OSPRey§	EML	E , L_i , and L_T	19	256	6.00	15.2	28.9	73.4	16.8	7.6
C-PHIRE	EAE	E_s and E_i	18	2,048	4.00	10.2	16.5	41.9	7.0	3.2
C-PHIRE	EPE	E_d	18	2,048	4.00	10.2	16.5	41.9	6.8	3.1
C-PHIRE	EPL	L_u	18	2,048	4.00	10.2	13.5	34.3	6.4	2.9
C-OSPRey	EAE	E_s and E_i	18	2,048	4.00	10.2	16.5	41.9	7.0	3.2
C-OSPRey	EAL	E , L_i , and L_T	15	2,048	4.00	10.2	20.3	51.6	7.6	3.4
C-OSPRey§	EAL	E , L_i , and L_T	15	2,048	4.00	10.2	24.3	61.7	8.2	3.7

§ Typically equipped with a removable shroud.

¶ Equipped with a permanently affixed shroud.

A comparison of the instrument systems influencing the C-PHIRE and C-OSPRey designs, along with their final physical specifications, are presented in Table 18 (with additional relevant material presented in Table 10). A shrouded C-OSPRey sun photometer is 51% lighter in weight than a corresponding OSPRey instrument. Although C-PHIRE E_d (EPE) and L_u (EPL) instruments are more than twice as heavy as the corresponding C-OPS instruments (XPE and XPL, respectively) with the radiance types being significantly heavier, the amount of weight involved is less than or equal to 1.7 kg per instrument. There are also generational differences in some instruments, which are briefly documented in Table 18, e.g., C-AIR versus the more advanced C-AERO.

9.3 Design

A harmonized design philosophy was used for the three primary categories of instrumentation uniquely associated with C-PHIRE instrumentation, as follows: a) the hybrid-spectral sensors, b) the ERI support electronics, and c) the HyPower2 boxes. Within the development, an emphasis was placed on designing the components such that they shared common characteristics allowing their application across the C-PHIRE (and C-OSPRey) instrumentation suite. The C-PHIRE instruments have a common bracket

set and support ring for mounting the CGS spectrographs between the end cap and the microradiometer cluster. Distinctions are made as required to adapt to the varied collector geometries deployed in C-PHIRE (and C-OSPRey), but otherwise the mounting scheme is portable between any instrument in the suite.

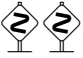
Similarly, the printed circuit assembly (PCA) designs for C-PHIRE are configurable for all instruments in the sensor suite. This allows the strategic inclusion or omission of components on an otherwise identical PCA. For example, the DC-DC converter required for powering the BioSHADE is included in a variant of the PCA used in the EAE, but omitted in the EPE where the converter is not required and potentially contraindicated due to its power consumption in battery powered scenarios such as SV3 deployments.

Additional PCAs were designed to perform multiple functions present in instrument subsets. For example, a single PCA is used to carry both Serial Peripheral Interface (SPI) data and analog temperature and depth signals. In embodiments not requiring these functions, the available space created by omitting the PCA is well defined and can be used for future developments or improvements. A similar approach was taken when new PCAs were required for both the ERI and HyPower2 variants.

In the C-PHIRE instrument suite, the microradiometer aggregator electronics were modified to allow seamless integration of high resolution temperature sensors. These miniature digital sensors are potted directly into the photodiode holder and monitor its temperature, thereby allowing more accurate temperature corrections to be applied to the acquired light observations. Expanding upon legacy instrumentation, the ERI and the radiometers that are part of the C-PHIRE instrumentation suite include physical ports for vacuum testing and dry nitrogen purging, as well as internal pressure transducers permitting continuous monitoring of the integrity of the housing seals. The latter is particularly useful for autonomous deployments, e.g., SV3 deployments of the TOW-FISH with solar reference (Sect. 8.8.7).

To further exploit efficiencies, a common 4 in (10.2 cm) OD aluminum tube with end cap was designed, which are used for both the C-PHIRE instruments and the ERI. This commonality allows the mechanical architecture to be easily expanded and modified for different instrument and accessory variations. Another area of harmonized design was in connector and cable selection. Whenever possible, connectors already in use with existing instruments (e.g., C-OPS and C-AIR) that have proven to be reliable (e.g., the SubConn micro series) were selected. This allows the efficient use of cabling and spare connector components that are presently available in field campaign mobilization assets.

One aspect of field mobilization that was not easily reproduced with the 13-conductor cable needed for extended USB communications was the concept that a small adapter cable should be used at the ends of cable runs, because this is the area of greatest stress (Hooker 2014). The rationale is that a short cable is less costly to replace and easier to have as a spare, than a long cable.

 For the 13-conductor Ethernet cable used with C-PHIRE instruments, the extra impedance associated with a cable connection prevents the addition of small sacrificial cables to absorb cable stresses at the mating ends, especially for longer cables where they will be the most beneficial, so extra care must be taken to ensure the ends of long 13-conductor cables are not subjected to detrimental and avoidable stresses.

9.3.1 Above-Water Irradiance (EAE)

From the perspective of standard radiometers (i.e., excluding C-OSPRey), the most complex radiometer is irradiance, because of the cosine collector and diffuser lens, so it was built first to ensure maximum lead time for unanticipated problem solving, with the following specifications:

1. The housing length is 16.5 in (41.9 cm) with a 4.0 in (10.2 cm) outer diameter;
2. The spectral range is 190–1,000 nm for the CGS and the spectral range for the microradiometers depends on the instrument system, i.e., 320–875 nm for TOW-FISH and 320–1,640 for C-OSPRey;
3. The spectral resolution is less than 0.4–2.2 nm for the CGS and equal to 10 nm for the microradiometers (except for C-OSPRey, the bandwidth at 1,245 is 15 nm and at 1,640 it is 30 nm).
4. The cosine response is 305–1,640 nm (the full range is used in C-OSPRey instruments);
5. The dynamic range is 10 decades for the microradiometers and about 4–5 decades for the CGS when not used in multi-pinned phase (MPP) mode;
6. The sampling rate is 15 Hz for microradiometers and varies by light intensity for the CGS (i.e., 15 Hz for E_s , 15 Hz at the surface for E_d that rapidly decreases with depth, and about 2–4 Hz at the surface for L_u that also decreases rapidly with depth);
7. The dark current corrections done for every CGS measurement use the UV pixels below 290 nm, and for the microradiometers caps are applied if possible or dark currents are obtained at night (moonlight permitting);
8. Thermal corrections may be applied for both the CGS and microradiometers;
9. Internal two-axis accelerometers determine the vertical orientation of the instrument;
10. The power PCA includes a complete module capable of supplying power to the shadow band and GPS accessories; and
11. The connector end cap includes a bulkhead connector to operate the shadow band and GPS accessories, and the end cap is configurable for multiple operational scenarios.

In regards to the connector end cap, for deployment on the SV3, the EAE bulkhead connectors are oriented at right angles to the end cap to accommodate the lack of vertical clearance; for C-OSPRey and shipboard C-PHIRE deployments, the connectors are mounted straight through the end cap to simplify cable routing and eliminate lateral strain on the cables and connectors.

A transparent view of the design of an EAE instrument is presented in Fig. 108. The components include the SPI and the microradiometer support electronics PCAs. The latter include the aggregator board the microradiometers plug into, plus the internal pressure, temperature, and humidity of the housing.

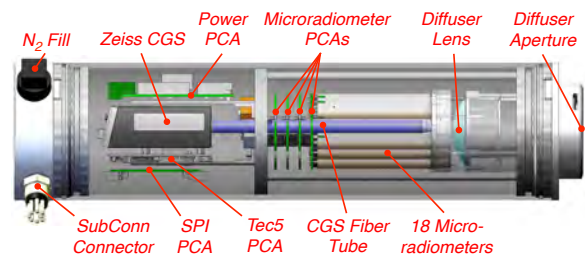


Fig. 108. The C-PHIRE above-water irradiance instrument design showing the major components.

9.3.2 In-Water Irradiance (EPE)

The in-water irradiance instrument (Fig. 109) is substantially identical to the above-water irradiance instrument (Fig. 108) used to measure the global solar irradiance. The design and configuration for both instruments is guided by the harmonized architecture conceived for the C-PHIRE radiometer development within the EPIC instrument class. The differentiations are intentionally minimized to exploit the economies and consistencies made possible by the development of the common instrument framework.

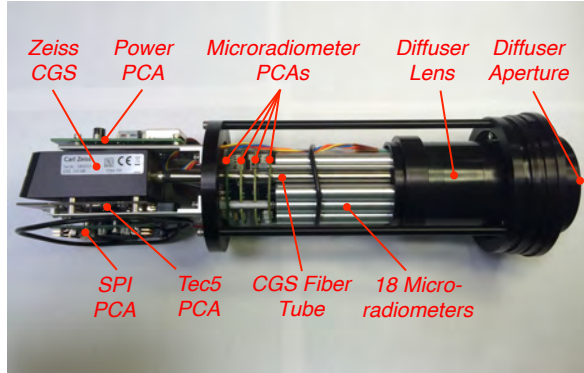


Fig. 109. The C-PHIRE in-water irradiance instrument design showing the major components.

Design differences between the EAE and EPE instruments are strategically asserted only as required to meet the scientific measurement requirements, or to provide tangible benefits for the anticipated scenarios associated with deploying the instrument as part of the instrument suite for which it is a part. Following this philosophy, the EPE is distinguished from the EAE by the following:

1. The EPE has a cosine collector that is optimized for use in water;
2. The housing is black rather than white to eliminate perturbations to the in-water light field because of reflected light from the housing tube;
3. The power PCA omits a large power supply module to reduce power consumption, favorably impacting mission endurance (the module is nominally used to power a shadow band and GPS accessory and is not needed); and
4. The connector end cap has a single bulkhead connector, because there is no requirement to support a shadow band and GPS accessory.

Following EAE cabling constraints, the EPE end cap connector is oriented at a right angle to the end cap to facilitate cable routing and prevent it from being exposed to damage outside envelope of the TOW-FISH backplane.

9.3.3 In-Water Radiance (EPL)

The radiance instrument adheres to the principle of a harmonized C-PHIRE architecture and is significantly

equivalent to the in-water irradiance radiometer with the following exceptions:

1. The housing length is 14.0 in (35.6 cm), versus 16.5 in (41.9 cm) for irradiance;
2. The radiance fore-optics assembly replaces the cosine collector and diffuser lens;
3. The CGS fiber tube has a smaller entrance diameter than the microradiometers, so it has a dedicated set of apertures to restrict the field of view (FOV) to be consistent with the FOV of the microradiometers;
4. The end cap contains the pressure transducer port and water temperature probe;
5. There are no tilt sensors; and
6. The end cap includes a bulkhead connector that connects the internal SPI PCA to the external altimeter.

The external altimeter provides a secondary and more accurate measurement of near-surface (upper 10 m) pressure and water depth, which is not harmed if the TOW-FISH descends to 10–100 m (the deepest depth is not possible, because the TOW-FISH sea cable is 35 m long).

When the digital thrusters on the TOW-FISH backplane drive the backplane to the surface, the altimeter and pressure transducer can be brought out of the water and tared, which means the uncertainties in water-leaving radiance, $L_W(\lambda)$, data products are lowered by as much as 0.5% for vicarious calibration and 1.0% or more for algorithm validation exercises).

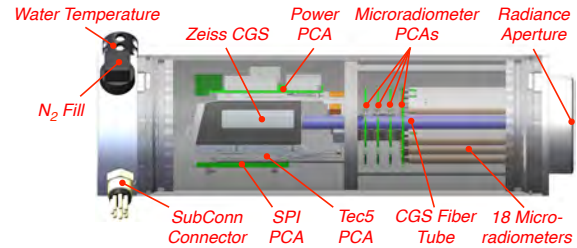


Fig. 110. The C-PHIRE in-water radiance instrument showing the major components (the pressure transducer port on the end cap is not visible).

The radiance fore-optics assembly FOV has a specified full view angle (FVA) that must be large enough to allow accurate measurements of all light sources, including low-light applications. The latter is not only broadband, e.g., moonlight, and includes spectral domains wherein light levels are inherently lower, e.g., UV flux during a plaque calibration. There are two preliminary engineering considerations that help define an optimized value for the FVA: stray light suppression and overall instrument length.

Stray light is less of an engineering issue for instruments measuring uniform light regimes with relatively low signal levels, e.g., in-water L_u measurements, which would not be the case for a sun photometer (C-OSPReY). Direct sunlight is several orders of magnitude brighter than sky radiance, so any contamination from stray light is maximal

when sky radiance is measured in close proximity to the Sun. Consequently, the design of the fore-optics assembly for the sensor includes baffling to control stray light.

A final engineering consideration is that the fore optics should not be more than 20 cm long to keep the overall length of the instrument within reasonable limits, because a shorter instrument can be deployed in more payload configurations than a longer instrument. These limits also need to be respected to ensure accurate pointing and control of the instrument, particularly for an instrument mounted on a backplane or tracker.

Minimization of the size of the instrument is also important for reducing wind loading (e.g., a solar reference on an SV3) and ensuring easier handling during servicing and the types of activities that take place during those events (e.g., monitoring the stability of a radiometer with a portable source). Although airborne applications frequently involve nacelles that shelter the radiometer from wind effects, compact instruments are typically easier to integrate and achieve flight certification than long instruments.

Above-water radiance radiometers are designed to measure the total radiance above the water surface, which is a combination of photons that have exited the air–water interface from below (i.e., are directly associated with the L_W signal), and photons reflected by the sea surface (e.g., glint from the sky and Sun). Waves, white caps, sea spray, plus sun and sky glint may lead to an inhomogeneous radiance within the FVA of the sensor.

Data points affected by glint and other factors can be filtered out, but only if the FVA is small and the sensor sampling rate is sufficiently high to discretize the contamination effects. This suggests that the chosen FVA should be as small as possible. From a practical perspective, this means an FVA in keeping with sun photometer design requirements. The FVA for above- and in-water C-PHIRE instruments, and as compared to other instrument systems, is presented in Table 19, wherein all FVA values are for the medium the instrument is designed to be deployed into.

Table 19. The FVA for above- and in-water sampling systems using C-PHIRE instruments and as compared to prior generations. For the FVA values, the SiP apertures are given with the CGS, as appropriate.

<i>Instrument System</i>		<i>FVA [°]</i>	
<i>Name</i>	<i>Model</i>	<i>SiP</i>	<i>CGS</i>
C-OSPREy	EAL	2.5	2.5
C-AERO	XAL	2.5	
C-AIR	XAL	2.5	
TOW-FISH	EPL	11.2	12.7
C-HyR	XPL	11.2	12.7†
C-OPS	XPL	11.2	

† The CGS accessory.

9.3.4 USB Extended and the ERE

The USB interface used for the cabling of C-PHIRE radiometers supports the necessarily high data volumes produced by the dual spectrograph and microradiometer detector systems. The combination of the use of the USB interface and the design goal of an instrument architecture that can be deployed both in close proximity to, and at a substantial distance (e.g., 100 m) from, a data acquisition computer requires provisions to overcome the inherent USB distance limitations, which is less than 5 m even in ideal conditions.

The technology selected to solve the USB cable-length limitation was used successfully in the C-HyR instrument development (Sect. 3.3.2). COTS USB Extenders developed by Gefen, LLC (Petaluma, California) were used to allow the C-PHIRE radiometers to satisfy the data and cable requirements for a variety of deployment scenarios. The technology allows the extension of USB 2.0 data telemetry over distances of up to 100 m using a single cable with data rates up to 480 Mbps.

A sender and receiver pair is required for each instrument location that is installed more than 3 m from the data acquisition computer. For the C-PHIRE instrument suite deployed on the SV3, the surface reference assembly is located in close proximity to the data acquisition computer, so only a single sender and receiver pair is required (i.e., one pair is needed for the in-water radiometers mounted on the TOW-FISH backplane). In comparison, the same C-PHIRE instrument suite deployed on a large research vessel, wherein both above-water and in-water instruments are likely located at the end of longer cables (up to 100 m) requires two sender and receiver pairs (i.e., one pair for the solar reference and one pair for the radiometers on the profiler backplane).

The USB sender modules (located in the HyPower2 box) are powered by the USB port in the data acquisition computer. The USB receiver module is integrated into the ERI and requires a separate power source, which is provided by the power PCA in the ERI. The extenders also have an integral four-port USB hub at the receiver module to facilitate the interconnection of multiple data streams. For example, for the TOW-FISH embodiment, the USB hub connects the two arrays of microradiometers, the two independent CGS spectrographs, and the pair of digital thrusters mounted on the backplane.

The EPIC class technology advancements achieved in the HARPOONS project were guided by the principle of a common architecture to enable flexibility in both instrument configurations and in realizable deployment scenarios compatible with other instrument systems. For example, one of the desired deployment configurations for the TOW-FISH with solar reference is to be able to deploy the instrument suite on a large research vessel in a fashion very similar to deploying a C-OPS with the Compact-Propulsion Option for Profiling Systems (C-PrOPS) accessory (Chap. 2), while recognizing that the larger size and

weight of the TOW-FISH backplane requires extra caution when lowering the profiler into the water and subsequently recovering it.

The configuration established for an SV3 deployment (Fig. 78), wherein the solar reference is sufficiently close to the HyControl box that a standard USB connection is suitable and the TOW-FISH cable connects directly to the HyControl box, presents three problems for deploying the equipment on a large research vessel in the same fashion that the C-OPS with C-PrOPS instrument suite is deployed, as follows:

1. The location for data acquisition is usually inside the ship and typically far away from the position on the deck where the TOW-FISH is deployed into the water, which means the sea cable must be extended to ensure as much of the sea cable can be deployed into the water as possible, rather than using a substantial portion of it to reach the HyPower2 box.
2. The solar reference on a large research vessel is frequently deployed using a Telescoping-Mount for Advanced Solar Technologies (T-MAST) and is likely too far away for a standard USB connection, plus the total cable length could exceed 100 m (e.g., on an ocean-class research vessel); and
3. The solar reference cable and the TOW-FISH sea cable must plug into separate HyPower boxes or a new HyPower2 box (i.e., a HyPower box with two cable ports), so the two instrument subsystems can be controlled and the data recorded (a HyPower2 box is preferred, because it is more space efficient from the perspective of positioning all of the equipment on limited bench space, which is a continuing concern in almost all deployments).

In regards to the anticipated requirement for a long solar reference cable, the routing of cables on a large ship can involve multiple diversions around obstructions to ensure shipboard safety equipment is not negatively impacted, e.g., going up and down to cross over walkways, going around life rings, going behind ladders, etc., all of which can consume an increasingly long length of cable (Hooker 2014).

To overcome the problems of deploying the TOW-FISH instrument suite on a large research vessel, wherein 100 m cable length restrictions or a requirement for segmented cable routing impose undesirable limitations, the EPIC Remote Extender (ERE) was designed and built. The ERE provides the ability to extend the total operational distance a C-PHIRE cable must traverse to 200 m from the data acquisition computer. All components are housed within an environmentally sealed case with waterproof connectors to allow the siting of the ERE in almost any outside location.



Shading the ERE from sunlight is desirable to prevent overheating of electrical components within the

sealed container, but in most situations this is not a factor, because the profiling measurements are typically short in duration.

The ERE (Fig. 111) passes the output power received from a HyPower box or variant (e.g., a HyPower2 or HyPower2+ box) through the ERE input to the ERE output, and repeats the communications channel to permit a doubling of the achievable USB extension distance.



Fig. 111. The ERE as an assembled unit with mounting plate affixed to the bottom of the waterproof case, which is removable.

Both TOW-FISH and solar reference distances may be extended through the use of two separate ERE units, but any individual cable must still be 100 m or less in length. The functionality is achieved by using the power delivered from the HyPower box (or variant) to the ERE to support a USB receiver and sender pair interconnected as a repeater, as well as to provide both internal and external visual feedback of when power to the system is on in the form of a highly visible blinking yellow light-emitting diode (LED).

The ERE can be secured in an organized fashion without obstructing access by crew or scientific personnel to safety equipment. A mounting plate made from ultra-high-molecular-weight polyethylene (UHMWPE) plastic was designed and fabricated as a generalized solution to provide mounting features allowing the ERE to be attached to a variety of surfaces and objects. The mounting plate is attached to the ERE using four stainless steel

screws which thread into a stainless steel plate that is bonded to the inside bottom of the ERE case. The mounting plate features a pattern of holes around all sides of the ERE case to allow screws or other fastening technologies to secure the case to a suitable fixture and it also functions as a heat sink to cool the interior electronics.

The ERE uses the same SubConn data series bulkhead connectors already used throughout the EPIC architecture at both the input and output, so no specialized cables are required. Consequently, cables procured to be used in conjunction with the ERE for a large vessel are valuable reinforcements to the spare asset pool for all EPIC activities.

9.3.5 The ERP

The ERP is the in-water profiler version of the ERI. Similar to the ERA, the ERP shares the 4 in (10.2 cm) OD form factor of the EPIC instrument-class architecture, but is 16.75 in (42.5 cm) long, and contains all required electronics to support EPIC instrument deployments at distances up to 100 m from the data acquisition computer. There are two primary distinguishing capabilities of the ERP relative to the ERA: a) the ERP supports both the power and telemetry requirements of a dual thruster architecture, and b) the ERP supports the simultaneous operation of two EPIC instruments, which is required for the TOW-FISH configuration.

The telemetry requirements of a dual thruster architecture are based on Recommended Standard (RS-485) specifications and are supported by a USB to serial converter at the integral hub of the USB extender receiver, which is routed through the combined power PCA common to the ERI architecture. The power for the thrusters is provided by a dedicated PCA that can supply more than 3 A to each thruster, if required. Operational thrust levels are typically kept well below this, i.e., typically 1–2 A, to maximize the lifetime of the thrusters. There are two bulkhead connectors provided for the thrusters, such that port and starboard thrusters each have a dedicated port.

Two dedicated bulkhead connectors on the ERP provide the physical interface for the two in-water EPIC radiometers mounted on the profiler backplane (usually E_d and L_u). These instrument ports are functionally equivalent, such that multiple cable routing options can be explored to best suit specific mission requirements.

Consistent with the HARPOONS philosophy of flexible and expandable system configurations, the ERP is designed to support the additional functionality described above while still receiving power and telemetry utilizing a single 13-conductor cable from any HyPower box variant (i.e., HyPower or HyPower2).

⚠️ ⚠️ A HyPower2+ may be used with an ERP with thrusters attached only for bench testing, because the HyPower2+ does not supply adequate power to support in-water thruster operation.

The sea cable used to connect to the ERP mounted on the TOW-FISH backplane has a terminated strength member. The latter distinguishes it from the cables used for handheld deployments, atmospheric investigations, and laboratory characterizations, wherein the strength member is typically not terminated.

⚠️ ⚠️ Tests of the first ERP module revealed a problem, wherein when thrust levels exceeded 30%, the thrusters created electronic interference, consequently, *electromagnetic interference (EMI) suppression was added to the thruster PCA and successfully tested to 120% of the maximum safe thrust level (50% thrust).*

Figure 112 shows the principal ERP electronics in obverse and reverse views. The figure also documents an escalating problem with connectors designed for consumer convenience, wherein extra securing mechanisms must be added to the instrument design. For example, the USB connection in Fig. 112 has added cable ties to act as keepers to help maintain the USB connection which only relies on friction to keep it secured, unlike the Registered Jack (RJ-45) ethernet connector with a built-in locking feature.

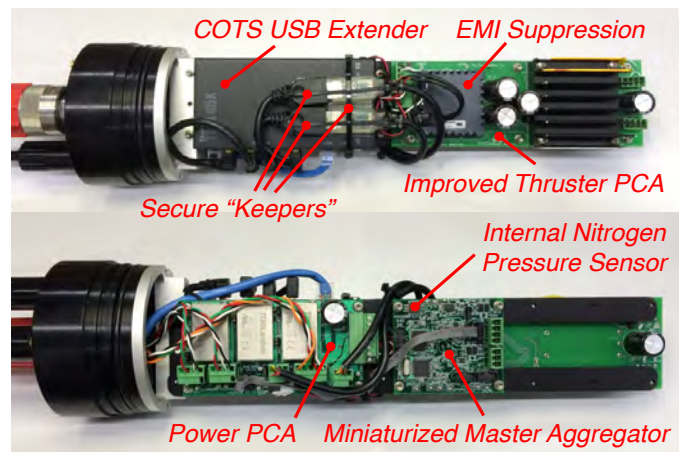



Fig. 112. The principal ERP electronics are the power PCA, miniaturized master aggregator, COTS USB extender, and improved thruster PCA with EMI suppression. Secure keepers ensure the USB connections do not part.

9.3.6 The HyPower2 Box

The principal difference between the HyPower box developed for the C-HyR profiler (Fig. 30) and the HyPower2 box is that the latter has two fully capable cable ports, wherein each port supports both USB extension and power delivery to an ERI connected to an EPIC instrument system, whereas the former has only one port and can only support one ERI connected to an EPIC instrument system. Each port has a dedicated USB extender allowing operational distances of up to 100 m and independent user-protection circuitry guarding against exposure to hazardous voltages. The power for the USB extender modules is nominally provided by the USB ports of the

data acquisition computer, but may be supplemented with external 5 VDC voltage supplies.

Consequently, the HyPower2 box can support both a profiling system with an ERP connected to two EPIC radiometers (E_d and L_u) plus an ERA connected to a solar reference system. In comparison, a HyPower box can support one or the other, but not both. This makes the HyPower2 box ideal for shore-based deployments, as well from small and large vessels, i.e., when it is desirable to deploy the TOW-FISH and solar reference in the absence of the SV3 from a ship, dock, or shoreline. The latter expands the range of operational scenarios available to science teams.

 The inventory of needed components to deploy the TOW-FISH and solar reference with the SV3 is not restricted to just the HyPower2 box; *it is also necessary to add an ERA for the solar reference.*

The picture of a HyPower2 box in Fig. 113 shows two USB extenders mounted on the front panel close to the hinge side of the waterproof case. The two ports are nominally labeled “PRO” and “REF” to provide an arbitrary (but logical) distinction. The three (red) connectors on the right edge (red) of the gray case are as follows (top to bottom): a) power (100–240 VAC); b) reference (port 2); and c) profiler (port 1).



Fig. 113. The HyPower2 box showing the two USB extenders (black with blue cables) and the displays (green) for the two cable ports (red, wherein one is for AC power).

9.3.7 The TOW-FISH

The TOW-FISH sea cable is the same one used with the C-HyR accessory (Chap. 3), except the strength member is terminated. The termination procedures are proprietary to the cable manufacturer, Teledyne Cable Solutions, formerly Storm Products, (Dallas, Texas), and are not presented here. Approximately 1 m beyond the strain relief of the sea cable trailing the SV3 Float, a 6 in (15.2 cm) oval yellow buoy is placed to keep the harness attached to the SV3 at the sea surface. The yellow buoy is a visibility aid for intended and incidental observers, and is the starting link in a chain of additional buoys to control the buoyancy of the sea cable in order to optimize the performance of the TOW-FISH.

A second 6 in (15.2 cm) oval yellow buoy is placed 2 m back from the first buoy, and a third one is placed 3 m back from the second. Additional buoys may be added as required depending upon operational conditions. For example, when the SV3 is operated in very calm seas, increased buoyancy may be desirable to keep the resting depth of the TOW-FISH closer to the nominal 5–6 m target. A principal benefit of maintaining the nominal resting depth is to prevent having to use extra thruster power to bring the TOW-FISH to the surface from excessive depths.

The TOW-FISH harness is similar in concept to the SV3 towing harness, and is oriented so the cabling extends beyond the radiance side of the backplane. This means when the sea cable is above the TOW-FISH during profiling, it is relatively far away from, and not obstructing, the E_d irradiance diffuser. A 4.5 in (11.4 cm) oval black buoy is secured close to where the TOW-FISH harness is shackled to the Kellems grip on the sea cable. This buoy prevents the shackle from sinking beneath the EPL radiance aperture and contaminating the light field.

Beginning 1 m from the strain relief on the sea cable at the TOW-FISH, five 1 in (2.5 cm) diameter cylindrical bladders that are 8 in (20.3 cm) long are installed in plastic mesh (Kellems grip) retaining sleeves and affixed at approximately 1.25 m intervals along the sea cable as it leads towards the SV3. The bladders fully expand at the sea surface, and fully compress before the TOW-FISH descends to the nominal 5–6 m resting depth. When the TOW-FISH is ascending, the slowly expanding bladders increase the buoyancy of the cable and assist in bringing the TOW-FISH and cable to the surface; when the TOW-FISH is descending, the slowly compressing bladders decrease the buoyancy of the cable and assist in sending the TOW-FISH and cable to the resting depth. The slow rate of compression improves the TOW-FISH loitering time and ensures high vertical sampling near the surface. The amount of bladders used can be varied to adapt to different operational scenarios wherein it may be desirable to modify loiter time and terminal descent rate convergence.

As part of the buoy integration activity, the oval yellow buoys selected for inclusion in the towing system were

modified to make the secure installation and removal of them at arbitrary locations along the sea cable trivial. The simplicity of the design allows the buoys to be easily attached or removed at sea by a swimmer. This enables operators to easily customize the buoy configuration beyond what is nominally located at each end of the sea cable in support of novel research or in response to challenging conditions in the field.

⚙️ To remove the necessarily periodic (and herky-jerky) motions imparted to the backplane during towing, *four isolation segments are attached to the sea cable a short distance from the backplane Kellem's grip connected to the TOW-FISH harness.*

In addition to sea cable buoyancy tuning, an isolation section to absorb sea cable stresses from towing dynamics is created using shock (i.e., *bungee*) cords. The design was conceived as part of mobilizing for the first Hawaii 2016 deployment off the Kawaihae coast. Four separate segments of shock cords with variable elongation resistance are installed along the sea cable between the locations of the compressible bladders described above at approximately 1.25 m intervals. The shock cords span a 0.75 m straight-line length within a longer sea cable loop (Fig. 114).

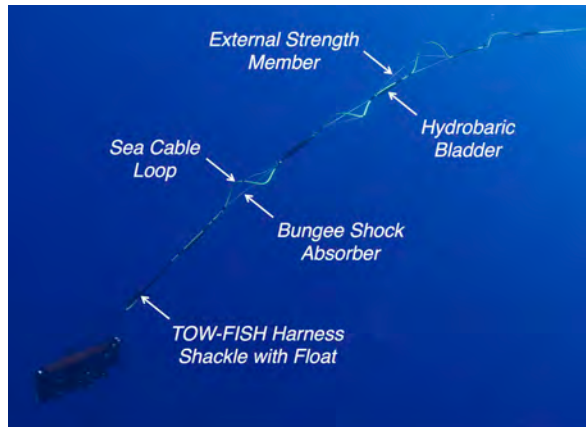


Fig. 114. The isolation section of the sea cable is positioned close to the TOW-FISH harness shackle.

The segment with the least elongation resistance is closest to the TOW-FISH, with each subsequent segment towards the SV3 having increased elongation resistance. The amount of elongation resistance is determined by the number of shock cords used to span the sea cable loops. This arrangement allows the strongest sections to absorb the bulk of the shock, and the sections of lesser elongation resistance to more delicately remove the remaining perturbations to the attitude of the TOW-FISH resulting from the pull of the SV3 float or the influence of the sea state.

When the SV3 Float is not moving forward, but the Sub is, there is no tension on the sea cable and all the sea cable loops are slack. Once the sea cable is brought under tension by the SV3 Float moving forward in the wave field, the shock-absorbing segments stretch starting

with the first segment, which has the most resistance. The segments continue to stretch in a cascading fashion, until the tension is completely absorbed. If properly configured, all four segments should rarely reach full extension, so the sea cable should rarely be completely taut.

Trials during both deployments in Hawaii established that the initial shock cord lengths were suitable for the oceanic swell encountered in Hawaii, and the strongest shock cord lengths were rarely fully extended. This proved to be primarily true during the Puerto Rico mission, but there was a relatively short period of time wherein the surface gravity wells developed to a larger amplitude than in Hawaii. Consequently, there was a short period of time when the shock cord lengths were fully extended.

During the SV3 training at the LRI facility in Kawaihae harbor, the LRI training team requested an external strength member for the TOW-FISH sea cable.

⚙️ To add another safety measure in the event of an accident that might cause damage to the sea cable, *500 lb (226.8 kg) breaking strength Spectra fishing line is routed from the Float harness shackle to the TOW-FISH harness shackle* (Fig. 79).

This component was retained during the field commissioning off Lana'i, as well as for the Monterey Bay and Puerto Rico deployments, because it was already installed.

9.3.8 The C-OSPRey Sun Photometer

The C-OSPRey instrument suite uses C-PHIRE radiometers, a quad detector for Sun detection, a PTU-D300 built by FLIR Motion Control Systems, Inc. (Burlingame, California) for tracking and pointing, plus support electronics (e.g., two ERA electronics modules and a HyPower2+ box). The solar reference system is an EAE radiometer fitted with a BioSHADE and Biospherical Global Positioning System (BioGPS). The sun photometer is a specially modified EAL fitted with a shroud and a filter-wheel assembly. Additional detailed information is provided in Chap. 10.

9.3.9 The CXL Transfer Radiometer

The CXR instrument system uses a single C-PHIRE EAL radiometer, ERA electronics module, and a HyPower box. A radiance instrument (CXL) was selected for the first embodiment of a CXR to complement the existing transfer radiometers used in the BSI calibration facility, wherein the OXL was scheduled to be retired. Additional detailed information is provided in Chap. 11.

9.3.10 DACPRO Software

DACPRO software was developed and deployed for both the TOW-FISH and C-OSPRey instrument suites. The capabilities include autonomous multi-day operations for data collection as described in Sect. 8.7.1 and Sect. 10.3.7, respectively.

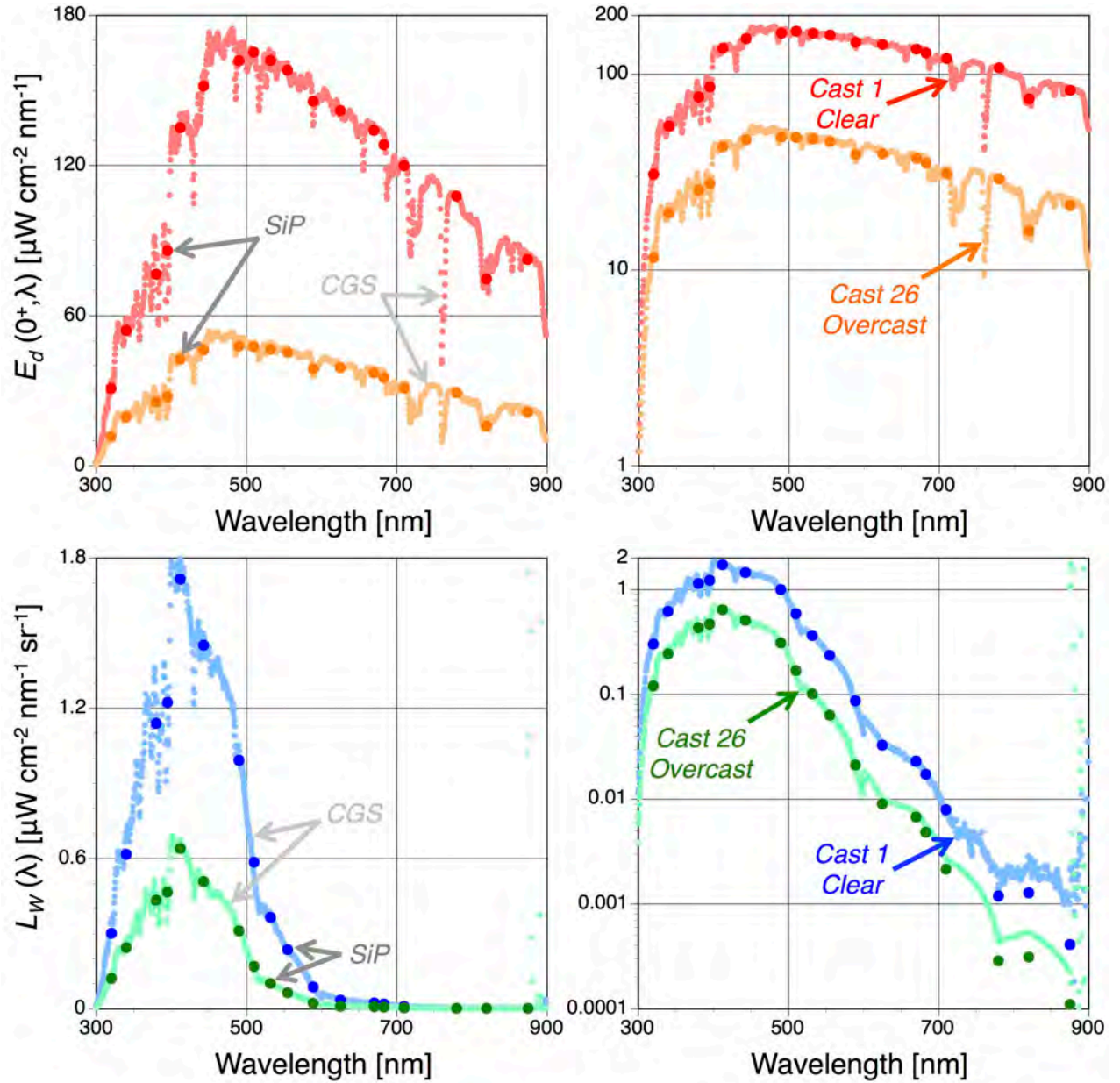


Fig. 115. Hyperspectral (CGS) and microradiometer (SiP) data for the global solar irradiance, $E_d(0^+, \lambda)$, plus $L_w(\lambda)$, for both linear (left) and logarithmic (right) y-axes. Kawaihae cast 1 and Lana'i cast 26 were obtained under clear and overcast sky conditions, respectively.

9.3.11 PROSIT Software

PROSIT supports the processing of TOW-FISH in-water data (with above-water solar reference data) and C-OSPReY above-water data as described in Chaps. 8 and 10, respectively. The CGS has 2,048 pixels spanning approximately 190–1,000 nm. Over the range used to obtain PROSIT data products, 300–900 nm, the native spectral resolution is 0.38–0.43 nm (UV–NIR). The SiP microradiometers span 320–875 nm (Table 10) with 10 nm bandwidths, so the significant overlap produces a robust hybridspectral detector system. Additional details are provided in Sects. 8.7.2 and 10.3.8.


9.4 Results

The PROSIT results from the first deployments of the above- and in-water SV3 instruments off the Kawaihae (cast 1) and Lana'i (cast 26) coasts are shown in Fig. 115. Casts from the earliest deployments are presented, so quality assessments can be applied to data from the very beginning of the activity. The sky conditions for the two casts are clear sky for cast 1 and overcast for cast 26.

For both casts in Fig. 115, the agreement between the SiP and CGS data is excellent throughout the UV and visible domains (300–700 nm), but the agreement between the CGS and SiP degrades in the NIR, as expected.

The anticipation that the CGS and SiP data products would show degraded agreement in the NIR is a result of the former having 4–5 decades of dynamic range and the latter having 10. Indeed, the reason why a hybridspectral instrument was built for the HARPOONS project was to ensure high quality data products in the NIR for vicarious calibration exercises.

One reason the CGS was selected for the C-PHIRE spectrograph was because the embedded CCD can operate in one of either two modes, which are referred to as non-MPP mode and MPP mode. The results presented in Fig. 115 were obtained from optical profiles with the L_u CGS operating in non-MPP mode. According to the manufacturer of the CCD, when it is used for repeated measurements over a short integration time, i.e., in a high flux level, the spectrograph should be used in non-MPP mode.

 As the flux level decreases, the integration time increases and, *ultimately, a limit is reached for non-MPP operation wherein for a long integration time, the dark current is problematic and the observations exhibit increased noise.*

This is one reason there is degraded agreement between the CGS and SiP detectors in the NIR domain in the Fig. 115 results.

Fortunately, the CGS provides a solution for noisy long integration times. In MPP mode, a voltage control is applied during integration, which greatly reduces the dark current and makes MPP operation suitable for integrations over a long period of time (i.e., suitable for low-light situations). Unfortunately, it was not possible to immediately use MPP mode for the L_u radiometer for the following reasons:


1. The documentation provided by Zeiss and tec5USA did not make the details of operating the CGS in MPP mode versus non-MPP mode completely clear with respect to anticipated in-water flux levels;
2. The Zeiss and tec5USA documentation required the radiometer to be returned for MPP configuration and optimization, and the subsequent use of a different device driver;
3. The documentation indicated the use of both MPP and non-MPP drivers at the same time might not be compatible on the same instrument suite, so it was possible all three radiometers would have to be in MPP mode, which posed unknown performance issues for the solar reference;
4. A device driver and DLL for operating the CGS in non-MPP mode was not available for Macintosh OSX, and creating one with limited help from Zeiss and tec5USA was sufficiently challenging that undertaking a second MPP device driver, with unknown DLL requirements, was not feasible until after the instrumentation first operationally demonstrated using the non-MPP mode.

9.5 Conclusions

After the SV3 with TOW-FISH and solar reference were successfully field tested as subsystems and a complete instrument suite (Sects. 8.8.1–8.8.3 and 8.8.6), then field commissioned (Sects. 8.8.4–8.8.5) and operationally demonstrated (Sect. 8.8.7), the TOW-FISH with solar reference was successfully deployed from a small boat, i.e., without the SV3 (Sects. 8.8.8). The independent deployment of the C-PHIRE instrument suite essentially followed the deployment practices for a C-OPS with C-PrOPS accessory, albeit the profiling package was larger and heavier.

The ability to deploy the TOW-FISH with solar reference from a small boat is an important achievement, because it provides a simpler platform for modifying and then testing the C-PHIRE instrument suite. For example, after the successful modification of the Macintosh CGS driver to support MPP mode, the L_u TOW-FISH radiometer was configured for MPP mode and then deployed in Lake Murray (San Diego, California). The purpose of the deployment (Sect. 8.8.11) was to obtain dark currents and in-water data for comparison with non-MPP data that had also been collected in a lake (i.e., Miramar Reservoir). Lake Murray was selected, because the time of the year (northern hemisphere winter) was not generally supportive of an offshore deployment, wherein high sea states are typical, whereas the lake was a sheltered environment with limited fetch.

The MPP data showed a significant reduction in the dark current in comparison with non-MPP data. Unfortunately the number of trials available under the limiting circumstances of the deployment, i.e., northern hemisphere winter with necessarily large solar zenith angles, did not allow for an adequate understanding of the optimal integration time to use in the relatively turbid water mass of Lake Murray.

 As integration time increases under large solar zenith angles, *the Lake Murray data also show that nonlinearities in response are possible if the integration time is too long.*

Consequently, the optimal water body for MPP trials is a clear water mass during cloud-free sky conditions wherein a higher solar flux does not require excessively long integration times.

Testing was also done to demonstrate that the harmonized but separated functionality of the SiP microradiometer array and CGS spectrograph within a C-PHIRE instrument means the device can be built without the spectrograph. The resulting standalone microradiometer sensor system would have no difficulty functioning, and the addition of the spectrograph at a later date would present no significant challenge. This two-step pathway for full implementation of the SiP and CGS detector systems provides a staggered costing approach, which might be beneficial for some applications. A three-step pathway is also possible by starting with a smaller array of SiP microradiometers and completely filling the array at a later date.

Chapter 10

The C-OSPRey Instrument Suite

STANFORD B. HOOKER
*NASA Goddard Space Flight Center
Greenbelt, Maryland*

RANDALL N. LIND, AND JOHN H. MORROW
*Biospherical Instruments, Inc.
San Diego, California*

JAMES W. BROWN
*RSMAS University of Miami
Miami, Florida*

RAPHAEL M. KUDELA AND HENRY F. HOUSKEEPER
*University of California Santa Cruz
Santa Cruz, California*

ABSTRACT

The C-OSPRey instrument suite leverages the harmonized design principles of C-PHIRE instruments while integrating previously demonstrated OSPRey capabilities. The C-OSPRey instrument suite was conceived to be deployed at a coastal facility near an in-water vicarious calibration site to provide supporting atmospheric observations and data products. A C-OSPRey system can be controlled by an operator or it can obtain measurements autonomously. The C-OSPRey system utilizes a quad detector for sun finding and sun tracking. A nine-position filter wheel in line with the spectrograph fiber allows the following measurements: three axes of polarization (0° , 45° , and 90°), dark offsets (opaque disk), bright-target (Sun) viewing with 3.0 and 1.5 ND filters, dim-target viewing (open), and improved stray light characterization (395 nm cut-on filter).

10.1 Introduction

The C-OSPRey instrument system was conceived to be deployed at a coastal facility near an in-water vicarious calibration site. It is designed to provide photometry measurements in support of atmospheric characterizations. If the shore location permits viewing of the sea surface absent platform-induced perturbations (e.g., from the top of a suitably configured offshore tower), water-leaving radiance observations can be derived from the solar reference data with contemporaneous sky and sea measurements (Hooker et al. 2002a and Hooker and Zibordi 2005).

A C-OSPRey system can be controlled by an operator or it can obtain measurements autonomously. The protocols for solar and lunar tracking, as well as the derivation of atmospheric data products from sky measurements, are provided by Hooker et al. (2012) and permit the derivation of many atmospheric data products, e.g., the aerosol optical depth (AOD), aerosol single scattering albedo (SSA), total column and precipitable water vapor (PWV), etc. The ratio of direct-to-global irradiance can be calculated

by comparison with the global irradiance measured by the companion solar reference.

The C-OSPRey design follows from the capabilities established with the OSPRey activity (Hooker et al. 2012), but in a more compact form factor. The C-OSPRey system consists of a radiance radiometer mounted on a tracker with a quad detector which allows the radiometer to be accurately pointed at the Sun and then to be pointed at targets with respect to the Sun. A companion irradiance radiometer equipped with a shadow band, GPS, and optional PAR sensor simultaneously measures the global solar irradiance (E_s) while the radiance instrument observes the selected target.

The anticipated measurements for the radiance instrument are as follows: a) the direct solar irradiance (E), b) the indirect sky radiance (L_i), or c) the total radiance at the sea surface (L_T). The PAR sensor is intended to facilitate autonomous operations, wherein observations would not be made if the PAR data indicated cloudy or rainy conditions. A schematic of the two subsystems is shown in Fig. 116.

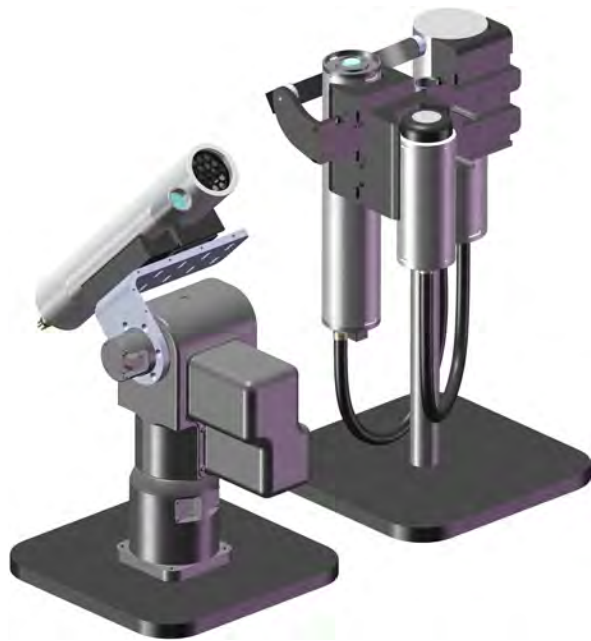


Fig. 116. A concept drawing of the C-OSPRey instrument suite showing the radiance radiometer on a tracker next to a smaller quad detector (left), plus the irradiance radiometer with shadow band and GPS accessories (right).

10.2 Background

The heritage for C-OSPRey is the OSPRey system (Hooker et al. 2012), which was designed to produce high-quality measurements of the sea, Sun, sky, and Moon across a wide spectral range, i.e., the UV-VIS-NIR, and SWIR domains. The design objectives were to provide vicarious calibration and algorithm validation capabilities to improve the following: a) the atmospheric correction of ocean color data, b) the accuracy in separating the living and nonliving components of seawater, c) the derivation of water-leaving radiances and associated data products in optically complex (coastal) waters, and d) the understanding of the interaction between the ocean and atmosphere.

Ancillary sensors broadened the characterization of atmospheric properties and safeguarded the sensors during severe weather or disabled acquisition during inclement weather. The measurements had a documented uncertainty satisfying the accuracy requirements for calibration and validation activities for both ocean color and atmospheric satellites. All optical measurements were traceable to the irradiance scale of the Spectral Irradiance and Radiance Responsivity Calibrations using Uniform Sources (SIRCUS) facility operated by NIST. The traceability was maintained with OXR instruments plus a lamp library of NIST and secondary lamp standards that is already established (Hooker et al. 2012).

A typical OSPRey instrument suite consisted of two radiance radiometers, each mounted on a pointing system or *tracker*, and two irradiance radiometers each equipped

with a shadow band to measure global and diffuse solar irradiance. The two pairs of radiometers, or *dyads* were a key design element of the OSPRey concept as was the modularity of the architecture. The latter allowed a system to be configured in the most cost-effective manner for the science objectives and available resources. For example, an OSPRey system may consist of only one radiance unit mounted on a tracker for the validation of satellite aerosol data products (a *starter system*), or the same unit might be deployed on an offshore platform with an irradiance sensor and also provide oceanic validation products (a *minimum system*).

OSPRey systems were built with EPIC instruments, like C-OSPRey, that were modified from the standard configuration as follows:

1. Redesigned radiance fore-optics for a smaller FVA of 2.5° in compliance with sun photometry requirements (World Meteorological Organization 2003);
2. Active thermal regulation to enhance filter and detector stability and reduce drift;
3. A new irradiance diffuser for the solar reference permitting a single cosine collector to span the UV to SWIR (305–1,670 nm); and
4. A radiance aperture removable shroud (Fig. 117).


 *The shroud ensures stray light contributions do not degrade data quality when viewing bright targets, especially at long wavelengths.*



Fig. 117. An OSPRey dyad making measurements at the Mauna Loa Observatory (MLO). The foreground radiometer is equipped with a removable shroud and the background instrument has no shroud (the solar references are not visible).

The OSPRey radiance instruments were also equipped with a digital video camera plus a nine-position filter wheel in line with the fiber-optic. The C-OSPRey instruments

use the same filter wheel. The filter wheel permitted hyperspectral polarimetry (three polarizers), direct Sun viewing (two ND filters), stray light correction (395 nm cut-on filter), and dark current measurements (solid disk). The digital camera was used in lieu of a quadrant detector to accurately point the sensor at the center of the Sun. The OSPREy trackers were the same military-grade COTS units used with C-OSPREy, and allow radiance radiometers to be pointed in arbitrary directions with a speed of up to 50° s^{-1} .

10.3 Design

The C-OSPReY instrument system (Fig. 118) was designed to leverage the harmonized architectural principles embodied in the development of C-PHIRE instruments (Sect. 8.3) while integrating relevant capabilities previously demonstrated in the OSPReY system. Compared to Fig. 104 showing the C-OSPReY instrument suite deployed on Mount Laguna, Fig. 118 emphasizes that the rather expensive buoyancy balanced yellow sea cable used for HARPOONS need not be used for C-OSPReY, although the cabling is compatible.

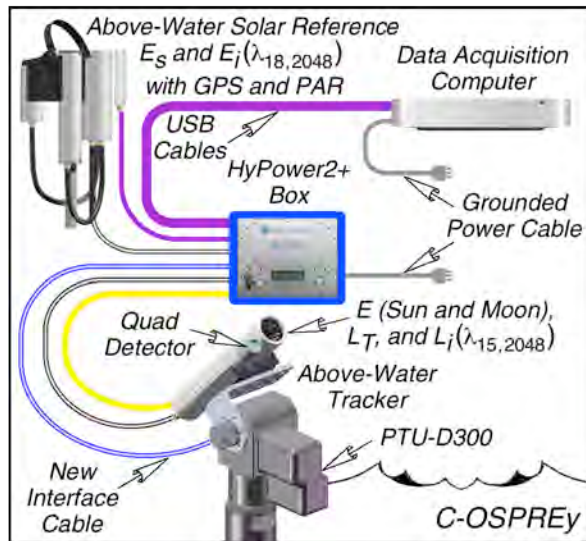


Fig. 118. The C-OSPRey system concept showing the above-water instruments, support electronics, and cabling required for data acquisition.

The mechanical and electrical architecture resulting from the C-PHIRE radiometer design allows a logical expansion path for the additional capabilities required for the C-OSPRey instrument. This philosophy also enabled the direct use of the ERA in the C-OSPRey system with no modifications or additional design effort, providing both value and flexibility for science teams in the procurement and maintenance of HARPOONS technologies both for active research and spare-component inventory. Similarly, the HyPower2+ box designed for C-OSPRey relies heavily on adapting the proven technologies designed and integrated for the HyPower (Sect. 3.3.3) and HyControl (Sect. 8.3.7) boxes.

A C-OSPRey sun photometer is the same instrument as an EPL radiance instrument (Sect. 9.3.3) with the following exceptions: a) narrower FVA (2.5° for C-OSPRey (versus nominally 12° for an EPL); b) nine-position filter wheel (versus no filter wheel); and c) 15 microradiometers rather than 18 (three microradiometers are removed to provide space for the filter wheel).

The C-OSPReY system utilizes a quad detector in its sun-finding and sun-tracking capability, rather than the digital camera used in an OSPReY EML instrument system, in order to provide a smaller, more robust, and flexible pointing system. A C-OSPReY instrument has the following additional differences (with respect to an EML):

- 15 microradiometers (rather than 19 for an EML);
- The Zeiss spectrograph has 2,048 pixels (versus 256 pixels for an EML);
- No active thermal regulation (EML radiometers are thermally regulated);
- HRT sensors to monitor the temperature of the photodiode holder, so more accurate temperature corrections can be applied to the acquired light observations (versus no such sensors for an EML); and
- A removable shroud rigidly mounted to the optical end cap (versus a concentrically mounted tube shroud for the EML).

The resulting size and weight differences of a C-OSPRey sun photometer with respect to an EML instrument are as follows:

- 4 in (10.2 cm) versus 6 in (15.2 cm) housing OD;
- 24.3 in (61.7 cm) versus 28.9 in (73.4 cm) long with shrouds; and
- 8.2 lb (3.7 kg) versus 16.8 lb (7.6 kg) weight.

10.3.1 The Sun Photometer (EAL)

The design for the C-OSPReY sun photometer (EAL) is based on the C-PHIRE profiler radiance (EPL) and the OSPReY EML instruments, with capabilities both added and omitted for the targeted applications of C-OSPReY. Specifically, the EAL has 15 microradiometers rather than the 18 of the EPL, and 19 of the EML. This is because, similar to the EPL, the fiber optic tube for the spectrograph is run through the microradiometer cluster. In the EAL, however, three of the microradiometers are removed to accommodate the nine-position filter wheel originally designed for the OSPReY instrument.

Like other C-PHIRE instrument suites, the EAL radiometer must be connected to a USB extender to allow for reasonable cable lengths during field deployments. In this case, the appropriate technology is an ERA (Sect. 10.3.5), which is the above-water atmospheric version of the ERI (Sect. 8.3.7). The ERA supports a single instrument system, like the C-OSPReY radiance radiometer.

The narrower FOV required for sun photometry was implemented by adapting the design of the fore-optics assembly with Gershun tubes and baffling from the OSPREy EML instrument. For the EAL, the filter wheel housing was redesigned so it mounts primarily within the diametrical constraints of the microradiometer cluster and its mechanical fixtures, as opposed to outside the microradiometer array as done in the EML. This required the removal of three microradiometers plus modified FOV baffle plates for the EAL fore-optics assembly to accommodate the substantially smaller active area (diameter) of the fiber now located within the cluster relative to the diameter of the window of the photodiodes used in microradiometers.

The relocation of the filter wheel enabled the EAL to be housed in a standard 4 in (10.2 cm) OD tube utilized in the harmonized instrument architecture (Fig. 119). This simplified the majority of the design effort by allowing the use of mechanical component interfaces already established for C-PHIRE instruments. Unlike the in-water EPL, the above-water EAL has a narrower FOV, a filter wheel, a fewer number of microradiometers, but a spectral range spanning 320–1,640 nm. The EAL also has a removable shroud that blocks stray light from reaching the entrance optics, which is needed for the more expansive spectral range of the EAL. In addition, the transducers and support circuitry required for in-water temperature and depth measurements are omitted from the EAL.



Fig. 119. The internal assembly of the C-OSPREy radiance radiometer from right to left, as follows: (black) gershun tubes, (silver) microradiometer array and filter wheel (colored wires visible), and (green) support electronics with CGS behind (partially visible).

Other important distinctions of the EAL with respect to the OSPREy EML are as follows:

1. The EAL has 15 microradiometers, whereas the EML has 19;
2. The EAL has the new Zeiss CGS spectrograph with 2,048 pixels, versus 256 pixels for the EML;
3. The EAL does not have active thermal regulation, while the EML had two levels of thermal regulation;
4. The EAL filter-wheel assembly was upgraded to include an encoder, and the EML had none; and
5. The EAL instrument is smaller in both the diameter and length, plus it weighs a little more than 50% less (as presented above).

From a physical perspective, the most notable differences between the EAL and EML, are the smaller size and lighter weight of the EAL.

10.3.1 The Shroud

The shroud for the C-OSPREy radiometer was adapted from the C-AERO instrument system. The mechanical similarities between the EAL and the exit optics for a C-AERO instrument allowed for the design to transfer seamlessly between the instrument families. The shroud is 2.75 in (7.0 cm) OD, 4 in (10.2 cm) long, weighs 0.6 lb (0.3 kg). It is internally *grooved* (Fig. 120) with knife-edge baffles to enhance the rejection of stray light. For comparison, the OSPREy shroud is 6.25 in (15.9 cm) OD, 6 in (15.2 cm) long and weighs 1.2 lb (0.5 kg).

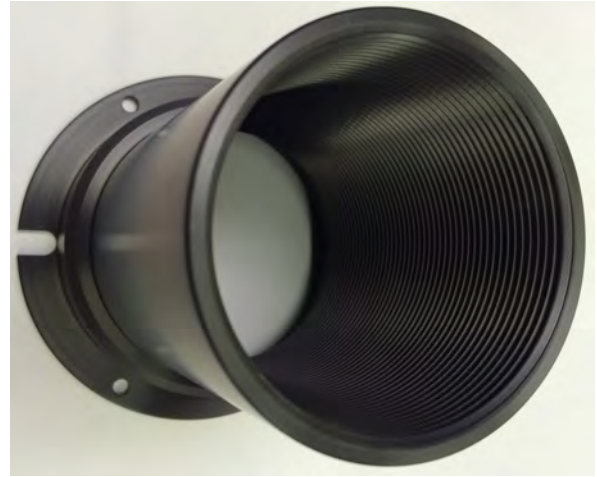



Fig. 120. The C-OSPREy removable shroud with internal grooves, wherein the larger diameter ring (bottom) mounts to the radiance aperture.

An important distinction between C-AERO and the C-OSPREy instruments is that the C-OSPREy shroud is removable from the EAL aperture.

 Because the C-OSPREy shroud is removable, *it cannot be used in deployment configurations that apply significant stresses on the shroud (e.g., airborne sampling) without a pre-flight analysis to certify the safety of the shroud and its attachment scheme.*

The ability to remove the C-OSPREy shroud permits easier cleaning of the glass aperture, a more compact shipping case, and facilitates comparison of measurements made with and without the shroud attached, in addition to permitting rapid experimentation with design refinements to meet evolving goals of the science team.

10.3.2 The OSPREy Filter Wheel

The C-OSPREy radiance instrument (EAL) was designed to use the same filter wheel as the OSPREy radiance radiometer (EML). The OSPREy nine-position filter wheel is mounted in front of the spectrograph fiber and uses an optical index (*home*) position to establish the following hyperspectral measurements: three axes of polarization (0°, 45°, and 90°), dark offsets (opaque disk),

bright-target (Sun) viewing (3.0 and 1.5 ND filters), dim-target viewing (open), and stray light correction (395 nm cut-on filter).

The OSPREy filter wheel measures 30 mm in diameter and is driven by a high resolution stepping motor controlled by the aggregator electronics. After construction, testing showed that the components are sufficiently light tight that high-quality dark measurements can be obtained by making the measurement in between two disk positions (except the home position). This frees up a filter wheel position for another purpose, if needed, because the opaque disk is not required for high-quality dark measurements. This extra functionality is not presently exploited.

When installed in the C-OSPREy EAL, the original OSPREy filter wheel is assembled in the redesigned housing and is mounted in line with the spectrograph fiber and within the array of microradiometers, as shown in Fig. 121 (a rotated close up of Fig. 119). The OSPREy embodiment has the spectrograph, fiber, and filter wheel mounted outside the microradiometer array in a larger housing, so it has 19 fixed-wavelength channels. For C-OSPREy, the microradiometer array is reduced to 15 channels to make space for the filter-wheel assembly and allows the instrument components to be fitted into a 4 in (10.2 cm) housing.

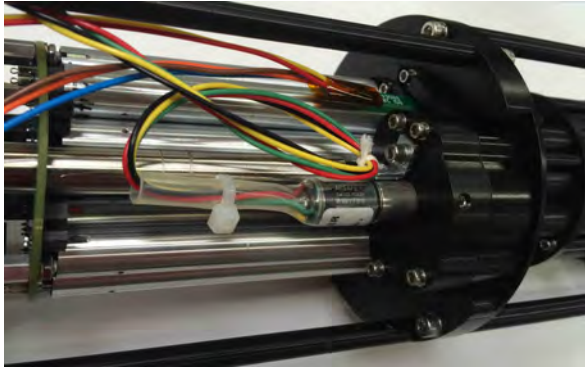


Fig. 121. The original OSPREy filter wheel assembled in the redesigned housing and installed in the first version of the C-OSPREy EAL radiometer.

10.3.3 The BioWheel

For the C-OSPREy radiance radiometer, the speed and reliability of the OSPREy filter wheel was improved upon through the development and integration of a new electromechanical interface to the filter wheel. This new accessory assembly is named the BioWheel and it is comprised of the filter wheel, a stepper motor, a micro-stepping motor driver, an absolute magnetic encoder, and an aggregator that is compatible with the microradiometer architecture.

The aggregator for the BioWheel appears in the data stream as a standard instrument aggregator and its data transmission contains the filter wheel companion data, i.e., the encoder count and the motor position. The companion data are required to correlate the position of the filter

wheel to the synchronous data acquired by the spectrograph. Similar to the C-OSPREy instrument and other instruments built with microradiometers, the BioWheel aggregator transmits data upon request to the ERA. The ERA merges both BioWheel and microradiometer components into a single data stream for the data acquisition computer.

Unlike the OSPREy design of the filter wheel, which was outside the array of 18 microradiometers (thereby necessitating a larger housing), the C-OSPREy design has the BioWheel mounted within the microradiometer array, as shown in Fig. 122, and fits within a smaller housing.

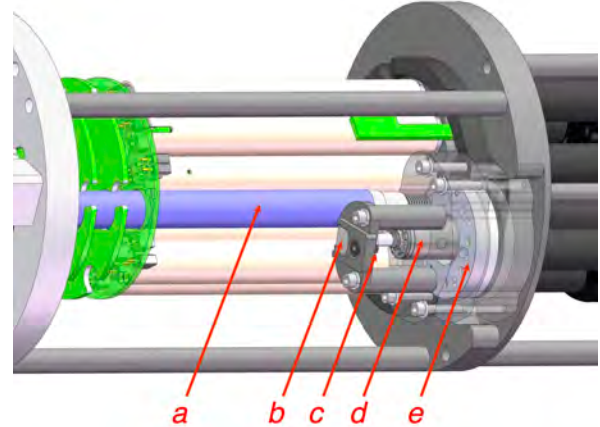


Fig. 122. A drawing of the BioWheel components installed in the C-OSPREy radiance radiometer, as follows: **a)** CGS fiber tube, **b)** encoder, **c)** encoder magnet, **d)** stepper motor, and **e)** filter wheel.

The upgrade of adding an encoder to the filter-wheel assembly enables science teams to maximize field opportunities by allowing simplified mobilization through a static filter wheel aperture position characterization as well as enabling more intra-day acquisition opportunities through the increased speed of the wheel. By exploiting the integrated absolute encoder, the BioWheel permits the correlation of the filter wheel aperture positions to encoder counts.

The aperture position characterization is performed in a laboratory setting and establishes a static relationship between wheel position and encoder value that is not impacted by short-term power cycling or longer-term inactivity (i.e., between campaigns). This capability improves reliability substantially over the OSPREy design, which required frequent optical homing with a stable light source, both of which increased mobilization complexity.

The CQM (Chap. 12) was utilized for the characterization of the BioWheel, though alternative stable light sources could be used if properly coupled to the instrument. The inclusion of a low gear ratio motor in conjunction with strategic microstepping increases the speed of the new filter wheel significantly, thereby allowing full rotations of the wheel in less than 5 s. In contrast, the OSPREy filter wheel required over 60 s to complete a full

rotation. This allows measurement sequences requiring different filters to be executed much more rapidly, expanding the number of acquisition opportunities in any given field scenario.

Although the filter wheel is the same as the one used in the OSPREy EML, the integration of the encoder improves its utility. Consequently, the BioWheel has more defined positions, resulting in an expanded nomenclature. The intent is to exploit the inter-aperture blocked positions for algorithmic efficiency in wheel movements, and is made possible by the detailed characterization created with the encoder. The wheel has a home position, 8 installable filter positions, and 7 intermediate positions where the beam is blocked, for a total of 16 positions (Table 20).

Table 20. The BioWheel positions and the corresponding measurement.

<i>Position and Measurement</i>				
0 Home	1 395 nm §	2 Dark	3 90° Pol. †	
4 Dark	5 45° Pol. †	6 Dark	7 0° Pol. †	
8 Dark	9 Opaque	10 Dark	11 ND 3.0	
12 Dark	13 ND 1.5	14 Dark	15 Open	

§ Cut-on filter (395 nm). † Moxtek polarization filter.

A look-up table generated during the characterization of the BioWheel correlates an optimal encoder reading to the center of the aperture in each physical position of the filter wheel. These encoder readings are subsequently used as the arguments for the command that moves the filter wheel to the specified position. Figure 123 shows the filter wheel mounted within the microradiometer array, with the filters numbered following Table 20. The even positions (not shown, except home, which is position 0) are in between the corresponding odd-numbered positions and can be used for dark measurements.

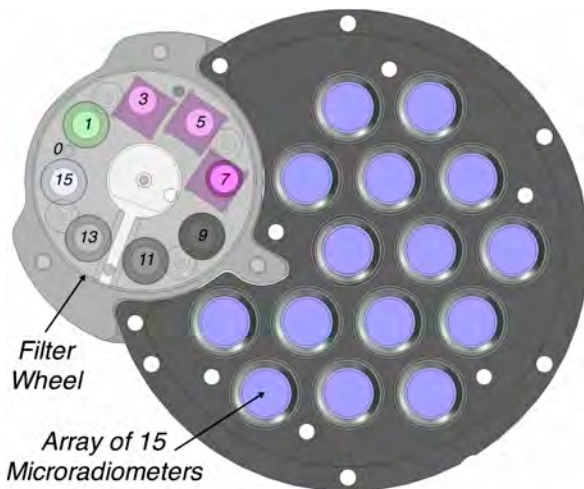


Fig. 123. The C-OSPREy filter-wheel assembly with a numbered subset of its assigned positions, as viewed from the external optical aperture of the instrument. Position 7 is in line with the CGS fiber.

10.3.4 The Solar Reference

The C-OSPREy EAE solar reference radiometer is essentially a duplicate of the TOW-FISH EAE solar reference mounted on the SV3 cover plate. The only significant difference is the specifications for the microradiometer filters. The C-OSPREy solar reference has an expanded spectral range that includes SWIR wavelengths and has three more microradiometers than the C-OSPREy radiance instrument, which were removed to make room for the filter-wheel assembly (Table 10).

Although possible, the C-OSPREy solar reference is typically not anticipated to be positioned close enough to the data acquisition equipment that the data can be acquired over a direct USB connection, as is done with the TOW-FISH solar reference (Sect. 8.3.1). Consequently, the C-OSPREy solar reference is connected to an ERA electronics module to allow cable lengths up to 100 m.

10.3.5 The ERA

The ERA (Fig. 124) is the above-water atmospheric equivalent of the ERI. It is nominally designed as an interface for a single EPIC instrument, but it is an expandable technology that could be adapted to support a dual instrument deployment to meet evolving goals of a science team. For example, a C-AERO (Sect. 1.4) deployment configuration using C-PHIRE instruments, which requires two radiance instruments and one irradiance instrument, could be supported with an expanded ERA for the two radiance radiometers and a single-instrument ERA for the irradiance radiometer (plus optional BioSHADE and BioGPS accessories). This evolution would allow for a more compact deployment configuration.

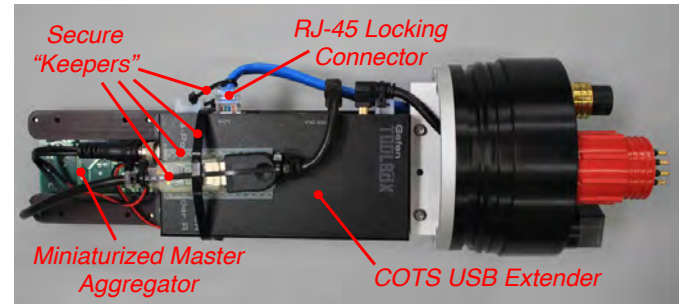


Fig. 124. The ERA with locking RJ-45 ethernet connector versus the need for additional secured “keepers” for the friction-fit USB connector (including the use of adhesive hook and loop tape).

The ERA shares the 4 in (10.2 cm) OD form factor of the EPIC instrument-class architecture, but is just 12 in (30.5 cm) long, and contains all required electronics to support EPIC instrument deployments at distances up to 100 m from the data acquisition computer. Consistent with the HARPOONS philosophy of flexible and expandable system configurations, it receives power and telemetry utilizing a single 13-conductor cable from any of the HyPower box variants (e.g., HyPower2 or HyPower2+).

The ERA integrates a PCA with a combined power supply for an EPIC instrument, spectrograph, BioSHADE, and BioGPS, along with a power supply for the extended USB communications interface and a master aggregator. It also includes the master aggregator PCA for consolidating microradiometer data streams, and a USB extender receiver module with an integral 4-port USB hub. The basic master aggregator includes power supply voltage and electrical current monitoring, along with a monitoring of the internal dry nitrogen pressure of the ERA housing, allowing software acquisition of data to provide confidence in the electronic function and mechanical integrity of the ERA. The latter is important to reduce risk for autonomous operations as envisioned for HARPOONS vicarious calibration activities.

10.3.6 The HyPower2+ Box

The HyPower2+ box (Fig. 125) is a specialized version of the HyPower box and is designed specifically for autonomous operation of the C-OSPRey instrument system. Like the HyPower2 box, it provides two ports that each support both USB extension and power delivery to an ERI connected to an EPIC instrument system. Unlike the HyPower2 box, there are power supplies and dedicated ports for the C-OSPRey PTU, quad detector, and PAR sensor. The power supplies for the EPIC instrument systems and the PTU are controlled by a DLP-IO8 interfaced to a custom HyPower2+ PCA using design concepts adapted from the HyControl box used with the SV3. In addition to enabling power switching, the HyPower2+ PCA allows the measurement of power supply voltage and electrical current, as well as monitoring of the internal temperature of the HyPower2+ box.

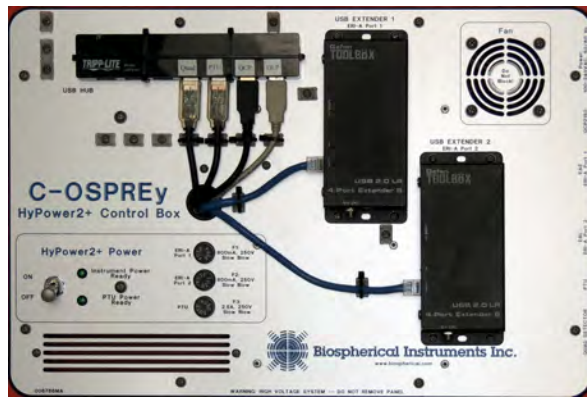


Fig. 125. The HyPower2+ control box panel showing the two Gefen USB extenders (black, right) and the Trip-Lite USB hub with four connections (black, left).

To simplify cabling, a powered USB hub mounted in the HyPower2+ box consolidates the data streams from the PTU, quad detector, and PAR sensor, while providing extra ports for future expansion. The instrument system data streams from the USB extenders are connected

to the data acquisition computer on dedicated USB cables. In-water systems with thrusters are not supported by the HyPower2+ box, because the available enclosure space usually reserved for servicing the additional power requirements presented in thruster-assisted systems is occupied by the power supply for the PTU.

The extra functionality of the HyPower2+ box requires three more bulkhead cable connections along the side than a HyPower2 box (Fig. 113), with assignments as follows (Fig. 125 right edge, top to bottom):

1. Power (100–240 VAC);
2. PAR sensor;
3. Solar reference irradiance radiometer ERA (port 1 USB extender);
4. C-OSPRey radiance radiometer ERA (port 2 USB extender);
5. PTU-D300 tracker and pointer; and
6. Quad detector.

10.3.7 DACPRO Software

The DACPRO software for C-OSPRey has two modes of operation, as follows: a) manual mode, wherein an operator makes data acquisition decisions and interacts with the software to activate and terminate data collection; and b) autonomous operation, wherein data collection is started and stopped following prescribed scenarios established before the instrument system is left unattended. Manual operations are usually associated with short-duration experiments, whereas autonomous operations are anticipated to support field campaigns lasting 10 d or more.

The autonomous capabilities include a system preference file for mission configuration, a daily schedule file describing when and how to collect data, a multi-day schedule file capability, power management of subsystems, management of data collection subsystems, periodic reporting of data collection activities, and periodic reporting of overall system status. Subsystems are powered on when required and otherwise stay powered off to conserve energy and reduce heating, which allows for battery-operated deployments. Another reason data collection subsystems are only used when required is to minimize computer overhead and memory usage, which minimizes fragmentation of computer resources. Data collected with DACPRO can be processed and visualized using PROSIT, which processes data on a cast-by-cast basis, wherein a cast is a file of data records obtained for a specified duration.

For C-OSPRey, a cast is obtained for a user-specified interval set in a daily schedule file that establishes the sampling period, which is typically 15 min (i.e., a cast is obtained every 15 min). There are multiple execution modes to obtain a cast. The two basic execution modes are distinguished by whether the aperture caps are on or off, with the former referred to as *light* cast and the latter

as a *dark* cast. Cast-specific behavior can be configured in a system preference file.

For a dark cast, the gain stages of the microradiometers are set sequentially to obtain dark current measurements at all gain stages, whereas for a light cast automatic gain control is used. For the spectrograph, dark data are obtained as a function of integration time, but during a light cast the integration time is usually set automatically.

Data collection during a light cast has five execution modes and is designed to support the derivation of the direct and diffuse solar irradiance, as well as the water-leaving radiance, as follows:

- Sun** Measurements of the direct solar irradiance are obtained with the tracker locating the Sun using the quad detector, and then tracking it during the acquisition time period;
- Sea** Measurements of the total radiance emerging from the sea surface are obtained after locating the Sun and then using the tracker to point the EAL radiometer perpendicular to the principal plane at a prescribed nadir angle (usually 40°) during the acquisition time period;
- Sky** Measurements of the indirect (diffuse) sky radiance are obtained after locating the Sun and then using the tracker to point the EAL radiometer perpendicular to the principal plane at a zenith angle equal to the sea-viewing angle during the acquisition time period;
- Shad** Measurements of the diffuse sky irradiance are obtained by rotating the shadow band across the solar the solar reference diffuser while the EAL radiometer tracks the Sun (i.e., makes a **Sun** measurement); and
- 4S** Sequential measurements of the Sun, sea, sky, and shadow band are obtained by executing the four measurements above (**Sun**, **Sea**, **Sky**, and **Shad**).


When a **Sun**, **Sky**, or **Sea** cast is executed, a **Shad** cast along with a second corresponding **Sun**, **Sky**, or **Sea** cast is typically performed. A **4S** cast performs **Sun** cast, **Sea** cast, **Sky** cast, and then a **Shad** cast followed by a **Sun** cast.

When a light cast is executed the sequence of steps are as follows (with the initiation and termination of all steps logged for status review and debugging, if necessary):


1. The cast is initiated by powering on the EAL and EAE radiometers, the PTU-D300, and the support electronics.
2. Data collection subsystems are started.
3. For a **Sun** cast, the PTU points the EAL radiometer at the Sun with the filter wheel positioned for the 3.0 ND filter (Table 20 and Fig. 123). For **Sky** and **Sea** casts the PTU points the EAL radiometer at the sky and sea, respectively, $\pm 90^\circ$ azimuth relative to the Sun with an open aperture (no filter). Data records are obtained for 70 s.

4. The shadow band is turned on, and a fast hemispherical sweep is followed by a slower return hemispherical sweep, which together take approximately 90 s.
5. Data collection subsystems are stopped.
6. The reference and radiance instruments are powered off, and the PTU-D300 is returned to the stowed position and powered off.

When the tracker moves the EAL radiometer, there is a so-called *dead band* in azimuth angles, which the tracker will not rotate across. If a desired $+90^\circ$ measurement is in the dead band, then -90° is used, and vice versa.

 *The dead band prevents the cabling that is connected to the tracker, EAL radiometer, and quad detector from coming under tension, which could result in data faults or damage to the instrumentation.*

A dark cast is similar to a light cast except the PTU does not move from the power up position and caps are assumed to be present on the reference and radiance instruments. The dark cast is initiated, and then data recorded sequentially at all three microradiometer gain stages and a series of spectrograph integration times. Data is collected for 70 s at each gain stage and 90 records are obtained at each integration time.

 *If the flux levels during a dark cast indicate the caps were on, a fault condition is triggered and the fault is logged.*

The acquisition software maintains a cast history log and also records diagnostic messages. A utility is available to create a cast log from the collected cast data.

10.3.8 PROSIT Software

The PROSIT application is used to process all data obtained from C-OSPRey measurements. The range of data products is a function of the types of casts that were made. For example, if **Sea** and **Sky** casts were obtained, one of the data products is the $L_W(\lambda)$ and its normalized forms. If **Sun** casts were made, the AOD is determined via the Langley technique or by applying the Beer-Lambert law to individual direct-normal measurements. Both methods are well established (Schmid and Wehrli 1995, and Schmid et al. 1999).

10.4 Results

The C-OSPRey instrument suite was field tested (Sect. 8.8.7.11) as part of the Puerto Rico Campaign to operationally demonstrate the SV3 with a C-PHIRE solar reference and the Float towing the TOW-FISH (Sect. 8.8.7). Despite generally poor atmospheric conditions over land during the periods when data were collected, the system performed within the nominal limits established for the field testing scenarios, plus sustainability and field maintenance were demonstrated.

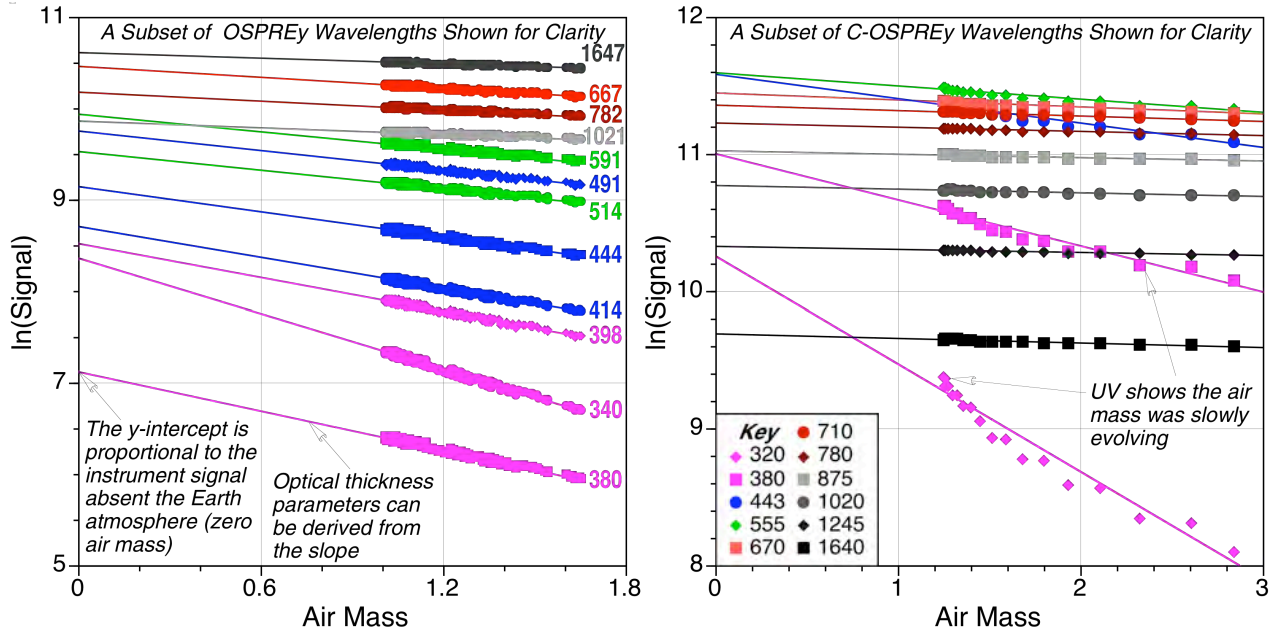


Fig. 126. Langley calibrations using microradiometer instruments, as follows: **a)** OSPREy on Mauna Loa (MLO) during 31 August 2012 (left); and **b)** C-OSPREy on Mount Laguna during 4 October 2017 (right).

Although University of Puerto Rico (UPR) maintains a Cimel sun photometer system, *the instrument was not functional during the deployment, which did not allow the planned direct comparison of the instrument with C-OSPREy*, although poor atmospheric conditions during C-OSPREy sampling periods would have limited the utility of the comparison.

The PTU-D300 tracker was field tested in San Diego (California) during the 21 August 2017 solar eclipse (Sect. 8.8.9). The minimum tracking value of the quad detector used for solar tracking is about 15% less than the anticipated direct beam from the Sun at the peak of the eclipse (about 60% occlusion). The DACPRO software successfully tracked the Sun during all phases of the solar eclipse.

The field commissioning of the C-OSPREy instrument suite took place on Mount Laguna (San Diego County, California) on 4 October 2017 (Sect. 8.8.10).

The proximity of the site to a large industrialized and heavily populated urban environment means it is not ideal for Langley calibrations.

The site has a clear eastern view of the rising sun elevation at an elevation of approximately 1,570 m (5,151 ft), however, so it was anticipated that the negative impact of lower-elevation atmospheric effects (e.g., the marine boundary layer) would be sufficiently reduced to provide reasonable field commissioning data. It was also close enough to BSI to make the mobilization options for measuring sunrise achievable.

A comparison of Langley calibrations obtained with OSPREy on Mauna Loa and C-OSPREy on Mount Laguna is presented in Fig. 126. The latter exhibit nonlinear

responses in the shortest wavelength (UV) channels (320 and 380 nm) that suggest the air mass was slowly evolving, whereas the former do not. The other wavelengths for the Mount Laguna observations have a linear response throughout.

The software refinement trials on the BSI rooftop in March 2017, included a day wherein the atmospheric conditions were clear and relatively stable. These data are used to compare the CGS with the SiP microradiometers. The CGS data have a finer spectral resolution, so the comparison is based on averaging the appropriate CGS pixels to within 1 nm of the SiP center wavelength to produce equivalent 10 nm bands (the potential 1 nm offset is in keeping with the determination of microradiometer filter center wavelengths). The comparison of the CGS 10 nm data from 8 March 2017 with respect to the matching SiP microradiometer data is shown in Table 21.

Table 21. A comparison of SiP microradiometer and equivalent CGS 10 nm bandwidth channels based on a Langley calibration obtained on 8 March 2017. The range of center wavelengths, λ_i in nanometers, exceed PACE[†] requirements (350–950 nm). The relative percent difference (RPD) values use SiP as the reference in the percentage calculations, i.e., $RPD = 100(CGS-SiP)/SiP$.

λ_i	RPD	λ_i	RPD	λ_i	RPD
320 [†]	4.6	555	−0.5	710	−1.8
380	−4.8	589	−1.1	780	−2.2
443	−0.1	625	−1.8	820	−2.7
490	−0.6	670	0.1	875	−1.8

[†] The comparison for 1,020 nm is −1.6%.


The Table 21 RPD values show all wavelengths agree to within the calibration uncertainty (Table 16) except 320 and 380 nm, which exceed 4.2%. The slightly elevated disagreement is not a significant concern, because as was the case for the Mount Laguna Langley calibration (Fig. 126), these data had higher variability in the UV and showed the air mass was evolving during the observations. This variability could likely account for the small differences (less than 1%) between the SiP and CGS observations.

10.5 Conclusions

The C-OSPReY instrument suite was designed to provide data products for Sun, sky, sea, and Moon viewing in support of oceanic and atmospheric research. It could also be used for terrestrial investigations, but this is not a focus of the science team developing and deploying the technology. The multiple uses of the instrumentation results in some compromised performance as a function of wavelength depending on the scientific objectives. For example, the center wavelengths and bandpasses of the microradiometers were chosen primarily to support ocean color research, which means they may not be optimal for atmospheric objectives.

If the Langley calibration data in Fig. 126 are used to compute the AOD, for example, there are issues with the microradiometer data that are perhaps best resolved by relying on the hyperspectral data, as follows:

- The steep decrease in ozone absorption within the 10 nm bandwidth of the 320 nm filter plus the temporal properties of the data (air mass is a proxy for time in Fig. 126) indicate ozone may have been changing during the period of the observations.

 *Deriving AOD at wavelengths influenced by gaseous absorption (e.g., ozone) requires filters with smaller bandwidths than those used with the C-OSPReY microradiometers, so some sun photometers exclude wavelengths below 340 nm.*

- The 820 nm microradiometer channel is in the middle of a water vapor absorption line.
- The 1,245 and 1,640 nm channels also have some interference with water vapor absorption, although the effect is smaller than at 820 nm, and the bias for the SWIR wavelength is likely acceptable.

In regards to the potential SiP bandwidth problem at 320 nm because of the steep decrease in ozone absorption within the 10 nm bandwidth, the presence of the spectrograph allows for the creation of data products with alternative bandwidths to overcome such problems. The nominal spectral resolution of the spectrograph in the UV is approximately 0.4 nm (Sect. 8.11.1). Ultimately, the hybridspectral design supports a more expansive set of science objectives across a wide diversity of applications.

AOD values derived from the data presented in Fig. 126 exhibit variations on the order of 0.05 over the time period wherein the measurements were obtained. While the variation is rather low, it shows that the day the Mount Laguna observations were obtained was good for making Langley calibrations, but not perfect. Whenever calibrations with the highest accuracy attainable are required, Mauna Loa is a preferred location, as shown in Fig. 126. Follow-on HARPOONS activities involving deployment of the C-OSPReY include plans for Langley calibrations obtained at MLO.

Chapter 11

The C-PHIRE Transfer Radiometer (CXR)

STANFORD B. HOOKER
*NASA Goddard Space Flight Center
Greenbelt, Maryland*

RANDALL N. LIND, AND JOHN MORROW
*Biospherical Instruments, Inc.
San Diego, California*

JAMES W. BROWN
*RSMAS University of Miami
Miami, Florida*

ABSTRACT

The CXR is a hybridspectral radiometer with an array of 18 microradiometers spanning 320–1,640 nm plus a 2,048 pixel spectrograph spanning 190–1,000 nm. The CXR is not temperature stabilized and is intended to be operated in controlled thermal environments. The first CXR is built in the radiance (CXL) embodiment, and is not expected to be used in the field. Instead, it is intended to be used in the laboratory to support the BSI calibration capabilities. The CXL replaces the OXL which was retired because of its age, more limited spectral range, and because the spectrograph was not compliant with next-generation mission activities.

11.1 Introduction

The evolution of the technologies integrated into all C-PHIRE radiometers provides the opportunity for a continuing advancement of measurement protocols. Without a well-documented and long-term effort to maintain standards of irradiance and calibrated reflectance targets for radiance, however, the temporal stability of both the radiometers and calibration sources is difficult to estimate and may add an unacceptable uncertainty to the measurements obtained with the field instruments.

With the development of the first hybridspectral radiometer, the EMR class, there has been an enduring perspective that representative instruments from each instrument class should be built and maintained as transfer radiometers for laboratory use. The resulting transfer radiometer instrument population provides essential technological and temporal overlaps to assist in the evaluation of the stability and efficacy of both new and existing calibration sources and radiometer classes. Because they are used repeatedly in controlled circumstances that are well documented, they provide important baseline information about the upper limit of expected performance of field instruments built within the same class of instruments.

Two transfer radiometers were built using the EMR class of instruments for the OSPREy activity. The radiance and irradiance OSPREy transfer radiometers were

designated the OXL and OXE, respectively. Both are thermally regulated and are based on combining the two different, but complementary, COTS detection capabilities within an EMR instrument. An OXR has a fixed-wavelength microradiometer array plus a hyperspectral spectrograph and is a standard EMR instrument. The hybridspectral design is similar to the C-PHIRE instruments built for the HARPOONS activity, wherein one microradiometer is removed so the spectrograph fiber can view the radiance aperture or irradiance diffuser.

The CXR is the latest-generation transfer radiometer designed specifically for the HARPOONS project and built in the radiance (CXL) embodiment. The CXL is a hybridspectral radiometer with an array of 18 microradiometers spanning 320–1,640 nm plus a 2,048 pixel spectrograph spanning 190–1,000 nm. Because it is a laboratory device, the CXL is anticipated to be used in a temperature-controlled environment and is not expected to be used in the field.

11.2 Background

The OXL, OXE, and the ground-based UV (GUV) transfer radiometer (XGUV) are legacy devices that have contributed to the long-term traceability and short-term evaluation of the BSI calibration facility. The XGUV is

based on PRR electronics and GUV-2511 radiometers, and has 12 channels. The XGUV is equipped with a cosine collector, is used on the irradiance optical bench, and has been in service at the BSI calibration facility for approximately 10 yr. It is temperature stabilized to within 0.1°C , and is optimized for UV transfers (six channels are in the UV), but still spans the NIR with a 290–875 nm spectral range. The spectral bandwidth of all channels is nominally 10 nm.

The individual lamp library standards used for BSI calibrations were originally characterized with the XGUV and OXL instruments. These radiometers can also be used to transfer irradiance scales from one lamp to another, e.g., from a NIST standard lamp to a working lamp. The OXL radiance instrument spans 340–875 nm with 18 microradiometers and 325–780 nm with a Hamamatsu model C9407MA (Bridgewater, New Jersey) spectrograph. The OXL is temperature stabilized to with $\pm 0.1^{\circ}\text{C}$, and the radiance fore optics have a 17° FVA. The spectrograph has a complementary metal oxide semiconductor (CMOS) detector with 256 pixels and 16 bit digitization, and the bandwidths are 7 nm in the UV and 5 nm in the visible. The OXL is normally mounted on the radiance optical bench.

The OXE irradiance instrument spans 320–1,640 nm with 18 microradiometers and 250–785 nm with a Zeiss Monolithic Miniature-Spectrometer (MMS) UV-VIS II device. The spectral bandwidth of the spectrograph ranges from 5–11 nm, and has a negative channel metal oxide semiconductor (NMOS) detector with 256 pixels and 15 bit digitization plus sign. The bandwidth of all microradiometer filtered photodetector channels is nominally 10 nm with the exception of the channels at 1,245 and 1,640 nm, which have bandwidths of 15 and 30 nm, respectively. The OXE is used on the irradiance optical bench.

The spectral response functions of the microradiometer channels in each transfer radiometer were measured with the BSI spectral tester (Bernhard et al. 2005) and their centroid wavelengths were calculated. The centroid wavelengths for the XGUV and OXL instruments are presented in Table 22 along with the new CXL, which replaces the OXL. The CXL has a spectral range that is more expansive than the OXL and almost the same as the OXE (Table 10). The bandwidth of all CXL microradiometer channels is nominally 10 nm with the exception of the channels at 1,245 and 1,640 nm, which have bandwidths of 15 and 30 nm, respectively. The OXL was retired because of its age, a more limited spectral range insufficient for PACE requirements, and because the spectrograph was no longer fully compliant with next-generation mission activities. Table 22 shows the CXL spans a larger spectral range than the OXL, both in terms of the microradiometers and the spectrograph, so the replacement transfer radiometer expands the capabilities of the BSI calibration facility. The OXE (Table 10) spans a similar spectral range as the CXL, is not as old as the OXL, and was not retired.

Table 22. Nominal (left column) and center wavelengths (all in nanometers) of the XGUV, OXL, and CXL radiometers used for lamp transfers including the HSG spectral range if present.

λ	XGUV	OXL	CXL
290	291.3		
300	301.1		
313	311.2		
320	319.9	318.2	319.5
340	339.1	339.1	339.9
380	379.9	379.3	378.5
395		395.6	
412		411.1	411.1
443	442.6	441.9	442.4
465		464.1	
490	489.1	489.0	489.9
510		509.3	508.2
532		530.4	
555	554.4	553.2	554.7
589		588.6	588.5
625		624.5	624.6
665	665.5	663.9	
670			670.2
683		683.0	682.9
710		708.1	709.9
780	779.5	777.6	779.4
875	875.1	873.4	875.4
1,020			1,017.8
1,245			1,244.2
1,640			1,639.9
HSG		325–790§	190–1,050†

§ 256 pixels.

† 2,048 pixels.

11.3 Design

The CXL uses the new CGS UV-NIR module, which is the result of collaborations between BSI and the manufacturer's representative, tec5USA, Inc. (Plainview, New York), and supplements OSPREy MMS modules. The CGS comprises an imaging grating, optical port, and a CCD detector with electric shutter to minimize integration times. The CGS is compact ($74 \times 30 \times 76 \text{ mm}^3$), thermally stable (which can be enhanced with added thermal regulation), and a full-width at half-maximum (FWHM) spectral resolution below 2.2 nm (UV-VIS) and 2.5 nm (NIR), i.e., approximately 2 nm.

The CGS spectrometer core is a blazed, flat-field grating for light dispersion and imaging. The CGS has excellent stability coupled with very low stray light and high reliability in rough environments. The CGS was selected based on exhaustive market surveys during the OSPREy project (2009–2012) with trade study refinements during C-HyR (2013–2014) development and subsequent operational demonstration (Sect. 3.4).

The design of the CXR instrument class was conceived to leverage the accomplishments of prior EPIC, C-HyR,

and C-PHIRE instrument development activities. In addition to sharing many common design elements, it is intended to be operable with all variants of the HyPower box that are part of HARPOONS instrument configurations. In conjunction with an ERA (Sect. 10.3.5), this allows a CXR to be operated at the same extended distances (i.e., nominally 100 m) from acquisition computers and power sources as other C-PHIRE instruments, such that any likely laboratory setting could be accommodated.

CXR instruments are not temperature stabilized, and are intended to be operated in controlled thermal environments. As part of the HARPOONS project, investigations of the detailed thermal characterizations for both microradiometer and spectrograph components in conjunction with the uniform structure of the spectrograph dark current suggest thermal and dark current look-up tables can be used to correct for small-scale temperature drifts encountered during operation.

From the perspective of thermal control, the small outer diameter of the CXR relative to the existing transfer radiometer population, 4.0 in (10.2 cm) versus 6.0 in (15.2 cm), provides adequate space for external temperature control of the CXR in thermally non-compliant settings. In addition, the thermal control architecture used for the CQM (Sect. 12.3.1) is applicable to the C-PHIRE instrument design and offers an innovative approach.

11.3.1 The CXL

A radiance instrument (CXL) was selected for the first embodiment of a CXR to complement the existing transfer radiometers used in the BSI calibration facility, wherein the OXL was scheduled to be retired. A picture of coincident CXL and OXL observations of a calibration plaque as part of retiring the latter for the former is presented in Fig. 127.

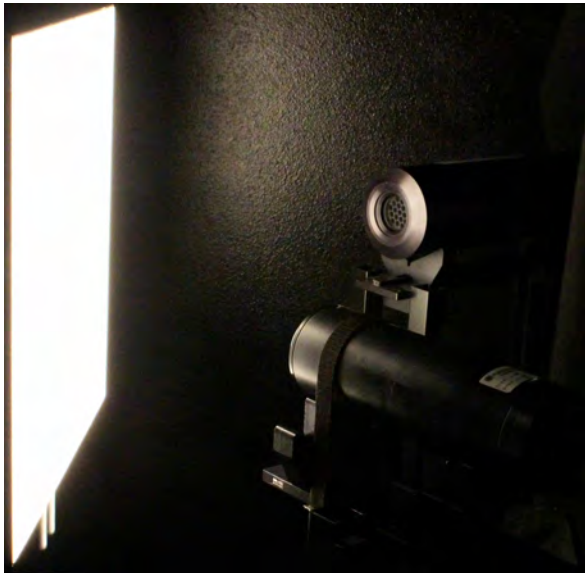


Fig. 127. Coincident CXL (foreground) and OXL (background) observations of a calibration plaque as part of retiring the latter for the former.

The CXL is consistent with the framework of the harmonized C-PHIRE instrument architecture (i.e., including C-OSPReY) and as such is intentionally largely equivalent to an in-water radiance radiometer, with the following distinctions:

- The microradiometer wavelength domain extends beyond the NIR and out to the SWIR (320–1,645 nm) to support a) calibration activities with the OXE (Table 10), b) lamp transfers out to longer wavelengths (Table 22), and c) instruments with wavelengths extending into the SWIR (Table 10), e.g., C-OSPReY and C-AERO;
- The end cap does not include a pressure transducer port and water temperature probe;
- The end cap does not provide for the connection of an external altimeter; and
- The end cap includes a single straight (as opposed to right-angle) bulkhead connector for power and telemetry, to facilitate cable routing in laboratory settings, wherein the right-angle connector seldom provides an advantage and is frequently a disadvantage.

Compared to the other radiometers in the C-PHIRE instrument suite, the CXL is subjected to significantly less deterioration, because it is only used in the laboratory. It is stored in a temperature stabilized calibration facility and as such is not exposed to the temperature gradients, weather effects, and physical shocks that field systems must necessarily endure, including when they are shipped. Consequently, the CXL represents a minimum endpoint as to the natural and inevitable consequence that aging imparts to instrument performance.

11.3.2 The ERA and HyPower Box

One of the important uses of the CXL for the HARPOONS project (Chap. 8) is to investigate the contributing factors to the long- and short-term stability and reliability of the HARPOONS instrument suite. In this investigation, the CXL is a primary source of data, because it is the only HARPOONS instrument that is not used in the field, so it is not subjected to environmental or shipping stresses. Consequently, the CXL can be compared to the C-OSPReY and TOW-FISH instrument suites, wherein the former and the latter two establish minimum and maximum thresholds for stability and reliability.

For the CXL to be used contemporaneously with the C-OSPReY and TOW-FISH radiometers for stability and reliability investigations, the latter two must be brought into a laboratory setting, which requires a laboratory light source. Because both radiance and irradiance radiometers are of interest to the investigation, a plaque and lamp combination is more cumbersome than simply using a portable light source like the CQM (Chap. 12), which has a compatible kinematic collar for both instrument types.

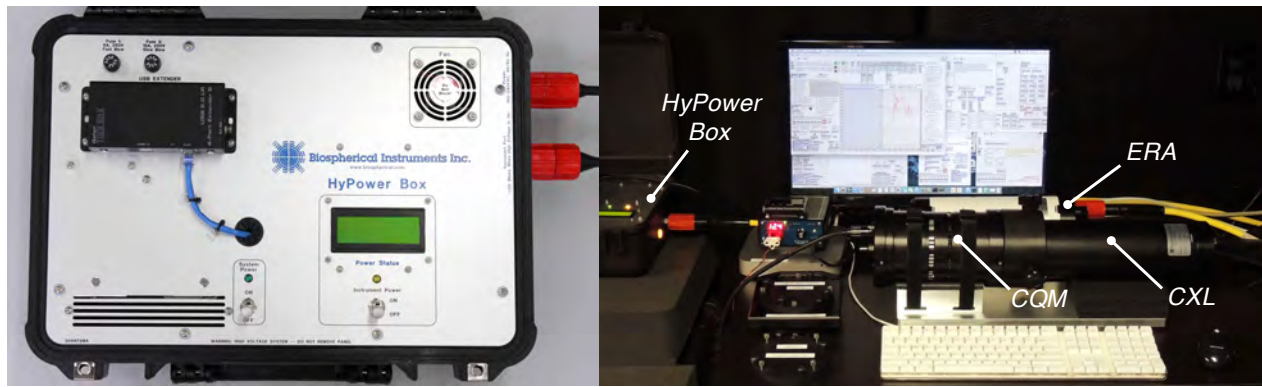


Fig. 128. A close up of the HyPower box (left), and the CXL in the laboratory cabled and powered with the ERA and HyPower box while observing the CQM light chamber (right). The background display shows the front panels for the DACPRO modules used to control the CQM and acquire the CXL data.

To be used without USB cabling restrictions, even in a laboratory setting, the CXL requires an ERA (Sect. 10.3.5) plus a HyPower box (Sect. 3.3.3) or one of its variants (Sect. 9.3.6 and Sect. 10.3.6). A close up of the HyPower box and a picture of its use in a laboratory experiment with the CQM configuration during CQM observations is presented in Fig. 128.

The small size of the CQM allows for compact experiments (compare to Fig. 127, which only shows the radiometers and the light source), but two instruments cannot simultaneously view the same light source. The excellent stability of the CQM makes this a minor concern. In addition, because the CQM exit aperture is affixed to the radiometer, there is a negligible opportunity for stray light to contaminate an experiment with the CQM (Chap. 12).

11.3.3 The DACPRO Software

The DACPRO software used to acquire data for the CXL is a subset of the virtual instrument (VI) modules used for all above- and in-water C-PHIRE instruments. A graphical user interface (GUI) provides the access to data acquisition execution modes wherein information streams from subsystems are combined in a single presentation of graphical depictions, calibrated variables, error status, data products, functional indicators, and control functions. The CXL is a laboratory instrument intended to support the BSI calibration facility, so the initiation and configuration perspective for the CXL is to support the calibration execution mode.

After the software is started and the SiP microradiometers are initialized, the hyperspectral CGS is started and the spectrometer is initialized. For each step in the data collection protocol, the calibration settings are set and the calibration execution mode button is used to initiate a timed data collection. Output files and directory pathways for each acquisition step have unique names created by an algorithm based on user-selected parameters regarding the devices and objectives of the data acquisition event, i.e., a single button is pushed with no other

required user interaction to record data (which makes automation straightforward).

11.4 Results

As part of the commissioning to enter the CXL into service for the BSI calibration facility, a laboratory activity was conducted wherein the CXL was positioned on the radiance calibration bench for repeated measurements of the reflectance plaque used as the source for spectral radiance calibrations. A working standard FEL lamp calibrated against a NIST standard of spectral irradiance was used to illuminate the plaque. The plaque was viewed at 45° and calibrated spectral radiance values were determined using spectral reflectance factors determined from the calibration provided by Labsphere, Inc. (North Sutton, New Hampshire).

Each session of the activity commenced by applying a computer-controlled current of 8.2 A to the FEL lamp and allowing it to stabilize for a minimum of 20 min. Concurrently, the CXL was powered on and allowed to stabilize for a minimum of 5 min. Modules of DACPRO software that were developed as part of the HARPOONS activity were used to control the configuration and recording of both the microradiometer and CGS spectrograph components of the CXL. The software recorded the following sequence of measurements from the CXL: dark capped data (at all three gain stages for the microradiometers), measurements of the plaque with the direct optical path from the FEL lamp to the plaque blocked such that only ambient (indirect) light reached the CXL, and measurements of the directly illuminated plaque. Three separate trials were conducted; between each of the trials, both the lamp and CXL were powered off, and the CXL was physically removed from the radiance calibration bench, so setup and positioning uncertainties could be included for each trial.

CXL stability during three observations of the BSI calibration plaque following the procedures above is presented in Fig. 129, wherein the CXL was positioned on the radiance bench using fixtures to ensure the correct distance

from the plaque and to ensure the instrument had the same rotational orientation during each measurement. The stability or reproducibility for each CXL wavelength in the radiance calibration is estimated by the RPD of the three measurements, which is computed as the observed value minus the average of the three measurements divided by the average with the quotient expressed as a percent.

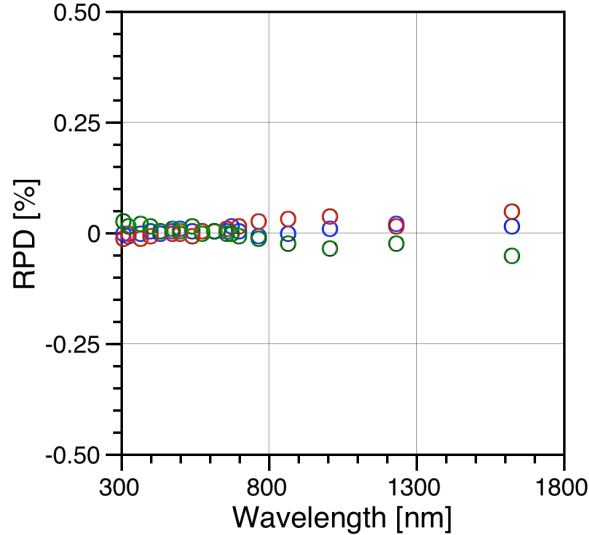



Fig. 129. CXL stability expressed as the RPD of three sequential radiance bench measurements (blue, green, and red) with fixtures for distance and rotational reproducibility.

Almost all of the data in Fig. 129 are to within an RPD value of 0.05%, which is an improvement with respect to the anticipated performance value of approximately 0.1% established by Hooker et al. (2002b). In addition to providing a stable radiometer, properly maintained reflectance plaque, and a stable operation of the lamp, minimizing variations in the distance between the radiometer and the plaque, as well as the rotational orientation of the instrument aperture, are requirements that must be satisfied if low RPD values are to be obtained. The most effective mechanism for achieving the necessary mechanical tolerances is through the use of fixtures that constrain the positioning and rotational orientation of the radiometer.

11.5 Conclusions

In the absence of using properly designed fixtures with mechanical stops to reproducibly constrain and position the radiometer during calibrations and characterizations,

undesirable variability—often in the form of avoidable biases that are typically not minimized by increasing the number of times a measurement is made—results in artificially brightened or darkened calibration coefficients, i.e., the instrument spectral responsivity has an increased uncertainty. Figure 130 presents three sequential radiance bench measurements wherein mechanical fixtures to ensure distance and rotational reproducibility during radiance calibration were not used.

 In this case, the CXL radiometer was positioned using visual indicators alone, e.g., a feature on the instrument housing was selected to point straight up to maintain the rotational orientation in the V-block used to hold the radiometer.

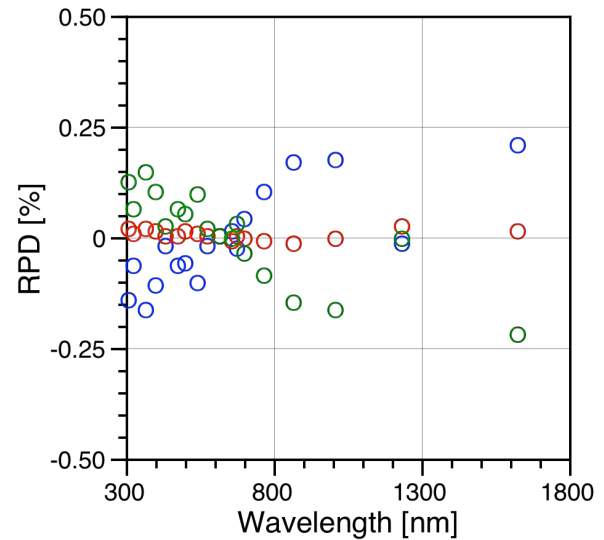


Fig. 130. CXL stability expressed as the RPD of three sequential radiance bench measurements (blue, green, and red) without the use of fixtures for distance and rotational reproducibility.

With respect to Fig. 129, the Fig. 130 data show an approximately factor of four overall increase in the RPD values, but not at all wavelengths. The microradiometer that is positioned in the center of the array is 625 nm, and the 625 nm data should be insensitive to changes in the rotational alignment of the instrument, which the data confirm. Microradiometers that are positioned closer to the center of the array, e.g., 1,245 nm, show less variance than microradiometers positioned farther away, e.g., 1,640 nm. Consequently, the use of properly designed fixtures is essential for controlling uncertainties during instrument calibration and characterization activities.

Chapter 12

The Compact Quality Monitor (CQM)

STANFORD B. HOOKER
NASA Goddard Space Flight Center
Greenbelt, Maryland

CHARLES R. BOOTH, RANDALL N. LIND, AND SHANNON T. WINCHESTER
Biospherical Instruments, Inc.
San Diego, California

JAMES W. BROWN
RSMAS University of Miami
Miami, Florida

ABSTRACT

The CQM is designed to provide stability monitoring in the laboratory and field with equal efficacy to track instrument performance between calibration activities with a stable light source in rugged, fixed geometric configurations. Compared to legacy light sources, the CQM uses LEDs rather than miniature tungsten filament bulbs as the light source. Like some legacy devices, three flux levels can be generated, but the CQM is substantially smaller and lighter while retaining all the required features of a portable source. C-PHIRE radiometers are built with a half-circle registration point on the edge of the aperture to allow a pin on the CQM to align the device in the same orientation each time it is used. To lower costs and allow rapid prototyping, the CQM relies on small COTS components whenever practical. The device can be operated in automatic or manual modes, with the latter including remote computer control over a serial connection.

12.1 Introduction

From the inception by Mueller and Austin (1995), the NASA Ocean Optics Protocols recommended the use of a portable standard to verify the stability of radiometers during deployment on research cruises, or other field deployments, of several weeks duration. This recommendation was based on limited experience with prototype analog sources developed by Austin and his colleagues in the 1980s at the Scripps Visibility Laboratory.

For the of HARPOONS project, the sequential deployment of the TOW-FISH and C-OSPRey instrument suites to support vicarious calibration activities would result in many weeks of deployment in the field before instruments were rotated back to a calibration facility. Even for a single deployment, if the time associated with shipping to and from a campaign site is included, even seemingly short missions as are applicable to HARPOONS activities, would benefit from stability monitoring, because of the stresses shipping can impart to the optical equipment.

Mueller and Austin (1995) included a discussion on tracking instrument performance in between calibration activities with stable lamp sources in rugged, fixed geometric configurations. The recommended specifications of the

device included the stability of the lamp output and the repeatability of measurement must be sufficient to detect 2% variations in instrument performance. In terms of the protocols for using the source, it was recommended that an instrument should be connected to the portable standard and its response recorded daily, keeping a record of instrument responsivity throughout an experiment. Furthermore, the use of a portable source should be designed to provide an essential warning of the onset or presence of problems if they appear.

One of the more important requirements in the use of the portable source was that it must be available when the complete radiometric calibrations are performed, so a baseline may be established and maintained for each sensor channel, but recognizing that the source cannot be a substitute for complete calibrations. The temporal record they provide will, however, be invaluable in cases where the pre-and post-cruise calibrations disagree or if the instrument is disturbed, e.g., opened between calibrations, subjected to harsh treatment during deployment or transport, or if the data quality are otherwise suspect. The use of a portable standards is an important part of the recommended instrument package.

12.2 Background

In 1995, an improved prototype of a portable source, the SeaWiFS Quality Monitor (SQM), was produced, and it proved suitable for use in the high-vibration shipboard environment (Johnson et al. 1998). The SQM was able to verify stability of radiometers with an uncertainty to within 1% and was instrumental in demonstrating that ion-deposition filters were required for radiometric stability to within 1% (Hooker and Aiken 1998).

After the development and deployment of the original SQM, less expensive versions of the device were made commercially available, e.g., the OCS-5002 built by Yankee Environmental Systems (Turner Falls, Massachusetts) and the SQM-II built by Satlantic Inc. (Halifax, Nova Scotia). Unfortunately, all of these instruments were not particularly portable and sometimes required substantial amounts of other equipment or laboratory space to stably power and maintain the temperature of the source.

Legacy sources were based on miniature incandescent light bulbs, which meant the spectral flux that was generated was frequently too low in the UV for the limited dynamic range of the instruments used at the time. Follow-on sources based on LEDs for illumination were also built. These sources had a significantly improved spectral shape of the light field, but were still rather cumbersome in regards to requiring a significant disassembly of an instrument to mount the radiometers into the source aperture.

12.3 Design

The CQM is designed to be more than 67% smaller than legacy portable sources and more than 75% lighter. It is 8.5 in (21.6 cm) in length with a 5.25 in (13.3 cm) outside diameter. The weight of the device without the kinematic coupler, bench top mount, or an attached device under test (DUT) is 6.0 lb (2.7 kg).

Although compact, the CQM retains all the required features of a portable source (Fig. 131), as follows:

- A thermoelectric cooler (TEC) mounted in the metal core printed circuit board (MCPCB) containing the LEDs;
- A digitally controlled fan to cool the heat sink, as required;
- A mounting arrangement wherein the entire CQM device fits onto a radiometer (i.e., like a dark cap);
- The sealed light chamber is walled with bead-blasted aluminum and fitted with a bead-blasted quartz window to ensure a homogeneous light flux; and
- The assembly is fitted into a vented shroud to protect the device, while allowing the fan to function.

An exploded (conceptual) drawing of the CQM is presented in Fig. 131. The *stacked* architecture of the components simplifies the design and lowers the development expense by not requiring a multitude of nonrecurring engineering costs to customize components or reduce the use of nonfunctional spaces.

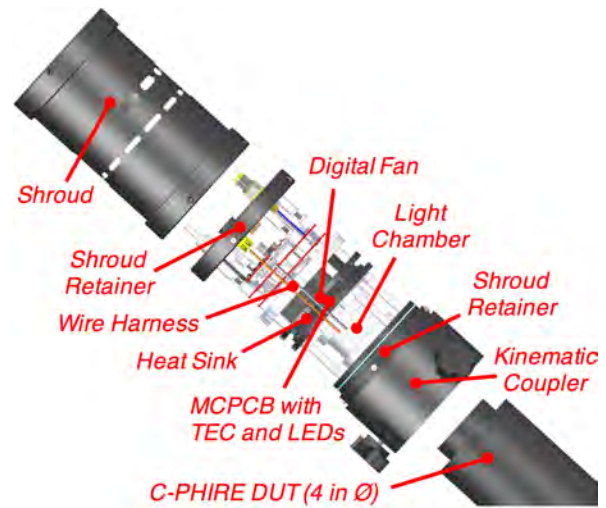
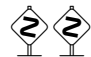


Fig. 131. A conceptual drawing of the CQM showing the subcomponents and alignment with respect to a C-PHIRE radiometer as the DUT and the kinematic coupler to secure the DUT to the CQM shroud retainer at the exit aperture.

Measurement repeatability and robust mounting of the DUT is accomplished using a kinematic coupler.

 The coupler incorporates alignment pins to ensure the DUT and the coupler are repeatedly used in the same orientation, and three radial coupler jaws secure the DUT to the coupler (Fig. 132).

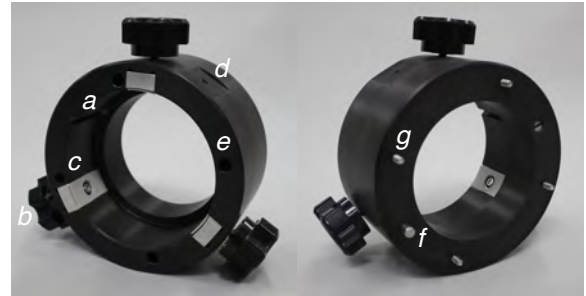


Fig. 132. Two views of the kinematic coupler to affix a C-PHIRE radiometer to the CQM showing the side that the DUT is positioned into (left) using the alignment pin (a) plus the three tightening screws (b) for the jaws (c) that securely hold it in place, wherein (d) provides an attachment point and counter-bored holes (e) allow access to 9/64 in socket head cap screws to secure the coupler to the CQM; and the side that is fastened to the CQM (right) with the alignment pin (f) and the four screws (g) to secure the coupler to the CQM.

The exposed surface of each jaw is covered with 1/32 in (0.8 mm) silicone rubber with a crisscross textured surface. The rubber barrier provides protection for the DUT against marring, as well as three secure non-slip contact surfaces around the DUT when compressed. Although Fig. 132 shows only one flat attachment point with hole



Fig. 133. The CQM MCPCB with electrical connectors on the outer rim and LED array in the center (left), which is mounted to a heat sink plus TEC within a cavity (middle), and the entire assembly is cooled with a digitally controlled fan (right). The images have different scales to distinguish different features.

on the kinematic coupler, a second one is located 180° radially from the first. Both holes have a 10-32 thread size to support mounting options for the CQM, DUT, and vessel or aircraft when the CQM is deployed in the field.

The kinematic coupler is installed using socket head cap screws that are located in counter-bored holes around the perimeter of the coupler. The targeted capability of measuring multiple instrument classes possessing outside diameters spanning the AOP instruments presently in use (including legacy radiometers) indicated that fiducials must necessarily be mounted to the shroud retainer rather than the DUT coupler. This arrangement ensures that the fiducial datasets recorded during measurement sessions are independent of the DUT geometry.

Three coupler options were created to allow the CQM to be used with different instrument diameters: 2.75 in (7.0 cm), 4.0 in (10.2 cm), and 6.0 in (15.2 cm). To overcome the awkwardness of legacy devices, which required the permanent attachment of a D-shaped collar to reproducibly insert the radiometer into the portable source, C-PHIRE radiometers are built with a half-circle registration point on the edge of the aperture to allow a pin on the CQM kinematic collar to align the device in the same orientation each time it is used. The kinematic collar also has a pin to ensure it is aligned to the CQM in the same orientation each time it is used.

12.3.1 CQM Hardware

To simplify the design and building of the CQM, and to create a prototype as inexpensively as possible, much of the architecture relies on small COTS components. The fan used for cooling, the TEC with thermoelectric control module, and the primary heat sink are all COTS items. The LEDs are mounted on a custom MCPCB, all of which are also commercially obtained (Fig. 133). The LEDs span the UV to NIR, and are divided into two sets with each supported by a constant current power supply. Each power supply can be turned on or off by program

control. Each power supply can be manually configured (some disassembly required) to output current in 20 mA steps from 20–100 mA in order to balance the output.

The use of an MCPCB for the LED array in the CQM is an innovation in AOP instrument design, which has application to other aspects of the C-PHIRE instrumentation. For example, versions of the C-OSPReY and CXR with temperature control are anticipated, and the circuitry needed to provide the feedback data for precise temperature control might involve sensors and circuits on a MCPCB with embedded TEC, as is done with the CQM.

A close up of the LED array used in the prototype CQM is provided in Fig. 134. The LEDs span the UV-VIS-NIR spectral domains and span approximately 365–940 nm, i.e., they provide a spectral range of flux that is nearly in keeping with next-generation Aerosols-Clouds-Ecosystems (ACE) and Plankton, Aerosol, Cloud, ocean Ecosystem (PACE) mission requirements.

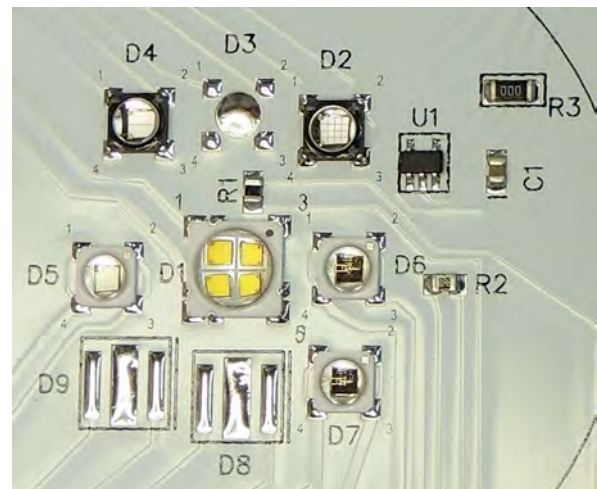


Fig. 134. The LED array on the MCPCB used in the CQM design. The largest LED in the center (D1) is a white LED that is made up of four smaller LEDs, which appear as four separately visible yellow-gold squares.

The broadest range of flux is achieved with the central D1 LED, which is actually four smaller LEDs (Fig. 134), and constitutes the first LED set. This large, white LED has a spectral range of 430–800 nm. The other seven LEDs (of which six are typically installed) constitute the second LED set and are used to produce a more complete spectrum using three in the UV and three in the NIR. The monitor photodiode at D3 and the LEDs at D8 and D9 are not installed in Fig. 134.


The D3 monitor photodiode, which is from the Hamamatsu S1336 series has a response spanning the UV to near IR that is suitable for precision photometry, as well as the D8 LED are visible in Fig. 135. Figure 135 also shows the CQM light chamber, with bead-blasted aluminum interior walls, during final testing after the initial testing documented in Fig. 134 was completed.




Fig. 135. The CQM light chamber showing the bead-blasted aluminum interior walls and a portion of the MCPCB.

There are also three temperature sensors on the LED board, for which one is a relatively low resolution digital sensor. There are also two thermistors. The first thermistor is digitized by a high resolution 24-bit analog-to-digital converter (ADC) controlled by the CQM microprocessor and its value is shown on the liquid crystal display (LCD) positioned on the back of the CQM (discussed below). The other thermistor is used by the temperature regulator.

A protective cap for the CQM light chamber plus two optical *fiducials*, one black and the other white, are supplied with the CQM. The surface of the white fiducial has a 0.25 in (6.35 mm) thick sheet of polytetrafluoroethylene (PTFE) for maximum diffused light reflection, and the dark fiducial has a hard black anodized coating. The cap is used to secure the light chamber from outside contaminants and protect the CQM during storage and transportation.

 *The reflective surface of a fiducial must be carefully maintained, both during use and when stored.*

Consequently, the reflective surface degrades very slowly and over the time period of a field expedition or laboratory time series, it remains essentially constant. In comparison to a fiducial, a field radiometer has a reflective surface that is changing episodically from the wear and tear of use in the field. The degradation in reflectivity alters the loading of the radiometer on the CQM light chamber and is a source of variance for the monitors inside the CQM that are viewing the light chamber, or the radiometer itself when it is viewing the light chamber.

 *CQM field and laboratory measurements must include the use of the fiducials, because the time series of internal monitor measurements with the fiducial in place gives an independent measure of the temporal stability and flux level of the generated light field.*

The protective dark cap and fiducials (Fig. 136), as well as the kinematic coupler, are all attached to the CQM using threaded holes on the face of the shroud retainer (Fig. 131) nearest the CQM exit aperture. For all of these components, the rotational orientation is reproducibly set by the presence of an integral alignment pin and a corresponding bore in the shroud retainer. After successful orientation of the alignment pin, the protective dark cap and fiducials are installed using self-retained thumbscrews.

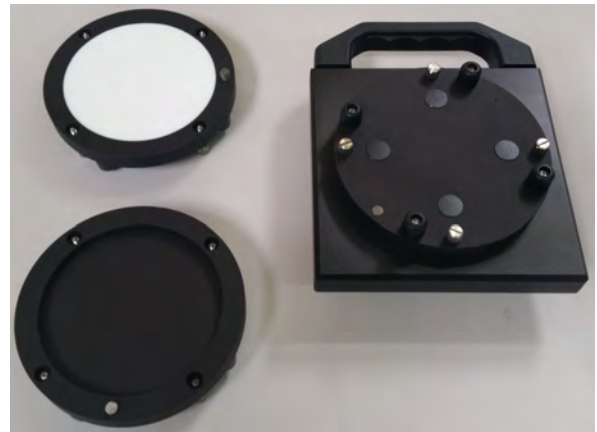


Fig. 136. The CQM white and black fiducials (left top and bottom, respectively) and the CQM exit aperture cap (right) with silver thumb screw heads visible (the fiducials are shown with the reflective sides, so the thumb screw heads are not visible).

The back of the CQM (the side opposite the quartz exit aperture) contains the following (Fig. 137):

- SubConn six-pin male micro series bulkhead connector for power and telemetry;
- Power switch, which provides 12 VDC (at nominally 1 A) to power the device;
- LCD, which can present 11 lines of diagnostic information concerning the function of the device;




- d) Mode select button, which also functions as an event marker, and allows control of the CQM, e.g., turning on either or both of the two sets of LEDs to illuminate the light chamber;
- e) Ambient temperature sensor; and
- f) USB memory port.

The power and telemetry cable is a standard cable used with many above- and in-water optical instruments, e.g., C-AERO and C-OPS. For the CQM, two conductors are used for the external 12 VDC power supply and the remainder for RS-485 telemetry. The latter allows remote control and recording of the CQM, e.g., with a computer.





Fig. 137. The CQM backplate showing the following: **a)** bulkhead connector, **b)** power switch, **c)** LCD, **d)** mode select button, **e)** ambient temperature sensor, and **f)** USB flash memory port.


The CQM may be powered by a laboratory power supply or a field deployable dedicated power box that contains a battery and power monitoring circuitry.

   The laboratory power supply used to power the CQM must have a current-limiting function to protect the CQM, in the event of a fault.

The mode select button (Fig. 137d) has two functions, as follows: i) if the button is pushed for less than 2 s, the operation mode of the CQM changes in a prescribed manner; ii) if the button is pushed longer than 3 s, an event mark is added to the data stream without changing the operating mode. The event mark allows the operator to correlate an important occurrence noted in a log with a precise location in the data stream.

  When using the mode button to change operating modes, it normally takes a data frame's duration to register the new operating mode.

When the CQM is powered on, operational parameters are loaded from non-volatile memory, the instrument starts up, several frames are recorded, and automatic operation initiates. Additionally, the RS-485 port transmits CQM serial opened and the LCD shows the most important operating parameters. If the mode select button is not pushed within 2 min, the CFM operates automatically with alternation of LED set 1, LED set 2, and dark segments.

 If the CQM is to be controlled remotely with a computer, the computer can take over the device at any time by issuing the appropriate commands over the RS-485 interface.

The following illustrates the use of the mode select button after successful start up, wherein the button is pushed once within the 2 min time period before automatic operation begins, which initiates manual operation with both LED sets off:


1. The first button push turns on LED set 1 (the high power white LED).
3. The second button push turns the white LED off, and LED set 2 (the UV and NIR LEDs) on.
4. The third button push turns on both LED sets.
5. The fourth button push turns off both LED sets.

A subsequent button push restarts the sequence with LED set 1 (the high power white LED) on.

When USB flash memory is installed in the external USB port on the CQM, it is automatically detected by the CQM, and a data file is created using the time stamp corresponding to when the CQM detected the flash memory.

 The USB port on the CQM is dedicated to the service of the flash memory; it serves no other purpose.

The CQM records all data frames generated by the CQM to the USB flash memory data file. All data records are comma separated ASCII text.

 Data generated by the DUT are not recorded to the USB flash memory, these data must be recorded separately.

The data frame rate is dependent upon the amount of averaging selected. When no averaging is selected, the data frame rate is approximately 0.4 Hz. These data frames are also output on the RS-485 pins of the CQM bulkhead connector for use by external software applications.

If the CQM is operated manually or by external computer control, the LCD is slightly different as shown in Fig. 138. Another difference shown in the figure is whether the LED sources are on or not. If on, colored vertical bars provide a visual representation as to the wavebands of illumination from the UV (blue) through the visible (white) and into the NIR (red).



Fig. 138. The LCD indicating the status of a variety of CQM parameters for automatic and manual operational modes (left and right, respectively).

The 11 lines available on the LCD for presenting diagnostic information include the following information from the top of the LCD to the bottom of the display, as follows:

1. The serial number of the CQM;
2. The firmware version;
3. The state of the LEDs;
4. The month, day, year, and time of the CQM real-time clock;
5. The number of records written to the data file on the USB flash memory drive, plus the input direct current (DC) voltage to the CQM;
6. The amount of time until the system transitions to the next LED stage during automated sequences, or manual operation indicator;
7. The monitor photodiode detector output;
8. The temperature measured by the thermistor on the LED board that is digitized by a high resolution 24-bit ADC controlled by the CQM microprocessor, and its difference relative to a nominal reference temperature programmed into the CQM;
9. Used for specialty purposes, and is blank when not in use;
10. The operating mode; and
11. The status of the USB flash drive or the data file name being recorded.

12.3.2 CQM Software

The DACPRO software environment provides two VIs to control and manage the operation of the CQM (additional VIs are used for the DUTs). The first VI, **CQM Ctl1**, manages the CQM RS-485 serial connection. This VI places the CQM in manual operating mode and sets the CQM clock to match the computer clock, which is nominally set to Coordinated Universal Time (UTC). All CQM operations data are recorded in hourly ASCII data files. Commands, responses, and other events are recorded in a daily ASCII log file.

The second VI, **CQM Main**, is the user interface to control CQM operation and data collection. The fan can be turned on and off, and the fan duty cycle can be set. Each of the two LED sets can be separately controlled. Run times for the LED sets are tracked for both the present session and cumulative overall sessions. Elapsed time for the present session is also displayed, but not recorded. Feedback is displayed for the LED state (e.g., on), fan speed, voltage for each LED set, and the currents for each LED set with instantaneous and averaged values (including standard deviation of averaged values).

The controls in **Calibration Settings** configure how the calibration data output file is named. The DUT control is used to select the fiducial (white or black) or the type of DUT. The S/N control sets the DUT serial number. The **Measurement** control describes the device and light configurations.

The execution modes provide four types of data collection. Hourly operational data are always logged, and the remaining three modes each record operational data into named files based on **Calibration Settings** as follows:

- count** A specified number of operational data records are recorded into the named file.
- time** Operational data records are recorded into the named file for the specified length of time, and is used during CQM warmup to record the operational data while the CQM light field stabilizes.
- cal** Operational data records are recorded into the named file for the specified time period, and is used to record operational data while DUT data are separately recorded using other VIs.

Normal practice is to set the fan duty cycle to 0.80 (80%), record the lamp warm up for 30 min, and collect 3 min of data for every measurement opportunity (e.g., each fiducial and each DUT). The DUT VIs also have **Calibration Settings** and execution mode **cal** so device data can be written to properly named files.

12.4 Results

To monitor radiometer stability in the field or laboratory, as well as CQM performance, a calibration evaluation and radiometric testing (CERT) session and a data acquisition sequence (DAS) need to be defined. In its simplest form, a CERT session is a sequence of DAS events, which are executed following a prescribed methodology. Each DAS represents enough data to statistically establish the performance characteristics of the DUT involved within a reasonable amount of time. In most cases for state-of-the-art and legacy devices alike, 3 min is sufficient.

A typical sequence of procedures for each CERT session is as follows:

1. The equipment for the operation of the CQM and DUTs is mobilized into the same location 1–2 hours before the CERT session begins to allow for environmental equilibration.

2. At least one DUT (preferably a laboratory radiometer like the CXL) should be designated a reference DUT and used in all sessions, particularly if the mixture of radiometers used in the CERT sessions are not the same over time. The first data collected during the CERT session should be the dark voltages for the reference DUT (usually achieved by putting an opaque cap on the radiometer) and the CQM internal dark voltages (usually acquired by blocking the CQM exit aperture with a cap or fiducial).
3. Once the CQM is powered on at the selected LED flux level(s), it is allowed to warm up for at least 30 min (but perhaps longer in highly variable environments). The total numbers of hours on each LED set are tracked by recording the starting and ending number of hours on each. The warm-up period can be considered completed when the internal CQM monitor data are constant to within 0.1%. The radiometric stability usually coincides with a thermal equilibrium as denoted by the internal thermistor.
4. Upon the completion of the warm-up period, the black then white fiducials are measured, and then the individual radiometers are tested sequentially. First, the previous DUT is removed and replaced with the white fiducial. Second, dark voltages for the radiometer to be tested and CQM monitor data for the white fiducial are simultaneously collected. Third, the white fiducial is removed from the CQM and replaced with the radiometer. Finally, data from the CQM and the radiometer are recorded. Each time a DUT is mounted to the CQM, the LED voltages and internal temperatures of the CQM are recorded.
5. If multiple flux levels are measured, and the present LED set is not to be used, it is powered off. The needed LED set is powered on and allowed to warm up for 30 min. The individual radiometers are tested sequentially and CQM fiducial measurements are obtained during dark voltage measurements (step 4).
6. Before the CQM is finally powered off, the white and then the black fiducials are measured. These measurements, plus the white fiducial data acquired in between the radiometer dark and light (CQM) measurements, are the primary sources for tracking the stability of the CQM flux. After the LEDs are powered off, the ending number of hours on each LED set is recorded.

It is important to note the warm-up process only involves the CQM and it is done once before the individual DUTs are measured; the DUTs are not warmed up *per se*, although, they are mobilized into the same room as the CQM 1–2 h prior to any measurements, so they are at room temperature.

The CQM monitor voltage is a direct measurement of the CQM light flux and its variability. An example commissioning trial of the stability in the CQM light flux

with both LED sets on is shown in Fig. 139, wherein the stability parameter is the RPD of the monitor voltage with respect to the overall mean as a function of time. During the trials to commission the CQM, the monitor voltage changed less than 0.1% during a 30 min warmup, as shown in Fig. 139.

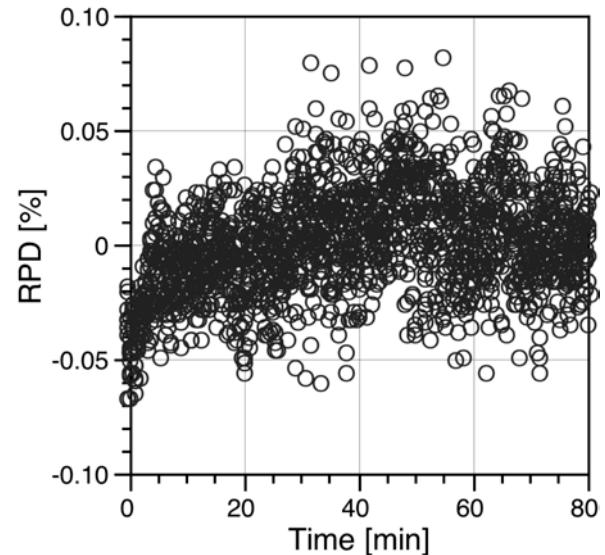


Fig. 139. A time series of the CQM light field with both LED sets on with the black fiducial and as observed with the CQM monitor.

During the stability trials for commissioning the CQM, the majority of monitor voltage changes occurred in the first few minutes of warmup. The monitor voltage varied within a 0.1% range once the 30 min warmup period completed, with most observations to within 0.05%. For the 0–30 min warmup period in Fig. 139, the average RPD is -0.12% , whereas for the 30–80 min period after that it is less than 0.1%. For the data in Fig. 139, after a 5 min warmup, seven measurements of C-PHIRE irradiance instrument EAE382 were made over the next 75 min. Each of these individual measurements had an RPD less than 0.1% relative to the average of all seven measurements.

If CERT sessions are conducted outside in the field, the CQM should be shaded from direct sunlight and ambient wind conditions to prevent rapid changes in heating and cooling. A major source of noise in the stability of the lamps is vibration, particularly if the CQM is used at sea. Vibration damping is recommended under such conditions and 0.5 in (12.7 mm) high density felt has been demonstrated to be a satisfactory damping material.

12.5 Conclusions

The three main components to monitor the stability of a radiometer with the CQM are shown in Fig. 140. For an instrument built with microradiometers, which is relatively light in weight compared to legacy devices, the radiometer is the heaviest component. For example, a

C-OSPRey sun photometer weighs 8.2 lb (3.7 kg), whereas the CQM weighs only 6.0 lb (2.7 kg). When all parts are assembled, the total weight is less than a legacy portable source alone, which weighed more than 45 lb (20.4 kg), i.e., without support electronics.



Fig. 140. The three main components for a CERT session: the DUT (left), the kinematic collar (middle), and the CQM (right). The precision DC external power supply for the CQM is not shown.

The Ocean Optics Protocols require the stability of the lamp output and the repeatability of measurement must be sufficient to detect 2% variations in instrument performance. To meet this specification, the design threshold for radiometric stability for the CQM was set to 0.1–0.2%, i.e., an order of magnitude lower. Based on the data obtained during commissioning the CQM, the thresh-

old for radiometric stability is to within 0.1%, as measured by the internal CQM monitor, and this is achieved within 30 min of powering on the LED set(s). In fact, the radiometric stability of the CQM immediately after powering on the LEDs (i.e., within 1 min) is also usually less than 0.1%, depending on the environmental conditions. Consequently, if a radiometer is subjected to some kind of trauma and needs to be checked as quickly as possible for an impending deployment, it is usually possible to check it to within reasonable limits using a rapid start of the CQM, particularly if the CQM is kept in a thermally stable environment.

The present device was built as quickly as possible and with the lowest-cost approach to establish the efficacy of the design concept. It was also built to distinguish the capabilities of the HARPOONS project as part of an anticipated follow-on vicarious calibration activity for next-generation ocean color missions that would further advance the technologies developed for HARPOONS, including the CQM.

⚠ Consequently, *the present CQM configuration does not provide a usable spectral response below 365 nm*, but the planned second-generation device will.

Another area for improvement is in the size and weight of the present CQM embodiment. The reliance on COTS components with simplistic connections and a *stacked* architecture means the device is not as small as it could be. Additional integration with customized engineering would shrink the total volume of the device and, thereby, reduce the weight.

ACKNOWLEDGMENTS

The high level of success achieved in the field work for the activities presented herein was the direct consequence of many individuals who contributed unselfishly. Their dedication is gratefully acknowledged. The captains and crew of the research vessels and aircraft who helped make the research a success are thanked for their professional contributions.

GLOSSARY

AC	Alternating Current	GmbH	<i>Gesellschaft mit beschränkter Haftung</i> , which means a 'company with limited liability and designates a private company in Germany.
ADC	Analog-to-Digital Converter	GPS	Global Positioning System
AOD	Aerosol Optical Depth	GSFC	Goddard Space Flight Center
AOPs	Apparent Optical Properties	GUI	Graphical User Interface
		GUV	Ground-based UV (radiometer)
BioGPS	Biospherical Global Positioning System	HARPOONS	Hybridspectral Alternative for Remote Profiling of Optical Observations for NASA Satellites
BioSHADE	Biospherical Shadow band Accessory for Diffuse Irradiance	HSG	Hyperspectral Spectrograph
BSI	Biospherical Instruments Inc.	HyPower	Hybridspectral Power (box)
		HyPower2	Hybridspectral Power 2-port (box)
C-AERO	Compact-Airborne Environmental Radiometers for Oceanography	HyPower2+	Hybridspectral Power 2-port (advanced box)
C-AIR	Coastal Airborne Instrument Radiometers	InGaAs	Indium Gallium Arsenide
C-OPS	Compact-Optical Profiling System	LCD	Liquid Crystal Display
C-OSPRey	Compact-Optical Sensors for Planetary Radiant Energy	LED	Light-Emitting Diode
C-PHIRE	Compact-Profiling Hybrid Instrumentation for Radiometry and Ecology	LRI	Liquid Robotics Incorporated
C-PrOPS	Compact-Propulsion Option for Profiling Systems	MCPCB	Metal Core Printed Circuit Board
CERT	Calibration Evaluation and Radiometric Testing	MLO	Mauna Loa Observatory
CMOS	Complementary Metal Oxide Semiconductor	MMS	Monolithic Miniature-Spectrometer
COTS	Commercial-Off-The-Shelf	MPP	Multi-Pinned Phase
CQM	Compact Quality Monitor	NASA	National Aeronautics and Space Administration
CXL	C-PHIRE Transfer Radiometer, Radiance	ND	Neutral Density
CXR	C-PHIRE Transfer Radiometer	NIR	Near-Infrared
DACPRO	Data Acquisition and Control for Photometric and Radiometric Observations	NIST	National Institute of Standards and Technology
DAS	Data Acquisition Sequence	NMOS	Negative Channel Metal Oxide Semiconductor
DC	Direct Current		
DUT	Device Under Test	OD	Outer Diameter
EAE	EPIC Above-water E (irradiance)	OS	Operating System
EAL	EPIC Above-water L (radiance)	OSPRey	Optical Sensors for Planetary Radiant Energy
EME	EPIC Multitarget E (irradiance)	OXE	OSPRey Transfer (radiometer) E
EMI	Electromagnetic Interference	OXL	OSPRey Transfer (radiometer) L
EML	EPIC Multitarget L (radiance)	OXR	OSPRey Transfer Radiometer
EMR	EPIC Multitarget Radiometer	PACE	Plankton, Aerosol, Cloud, ocean Ecosystem
EPE	EPIC Profiler E (irradiance)	PAR	Photosynthetically Available Radiation
EPIC	Enhanced Performance Instrument Class	PCA	Printed Circuit Assembly
EPL	EPIC Profiler L (radiance)	PROSIT	Processing of Radiometric Observations of Seawater using Information Technologies
ERA	Epic Remote Above-water (interface)	PTFE	Polytetrafluoroethylene
ERE	EPIC Remote Extender	PWV	Precipitable Water Vapor
ERI	Epic Remote Interface	RPD	Relative Percent Difference
ERP	Epic Remote Profiler (interface)	RJ	Registered Jack
FOV	Field of View	RJ-45	Ethernet Connector
FVA	Full View Angle	RS	Recommended Standard
FWHM	Full-Width at Half-Maximum	SiP	Silicon Photodetector
FWL	Fixed Wavelength	SIRCUS	Spectral Irradiance and Radiance Responsivity Calibrations using Uniform Sources
		SPI	Serial Peripheral Interface
		SQM	SeaWiFS Quality Monitor
		SSA	Single Scattering Albedo
		SV2	(Unmanned) Surface Vessel 2 nd (generation)
		SV3	(Unmanned) Surface Vessel 3 rd (generation)
		SWIR	Short-Wave Infrared

T-MAST Telescoping-Mount for Advanced Solar Technologies
 TEC Thermoelectric Cooler
 TOW-FISH A Towable Optical Wave-Following *In Situ* Hybrid
 UHMWPE Ultra-High-Molecular-Weight Polyethylene
 UPR University of Puerto Rico
 UTC Coordinated Universal Time
 UV Ultraviolet
 VAC Voltage Alternating Current
 VI Virtual Instrument
 VIS Visible
 XAE XTRA Above-water E (irradiance)
 XAL XTRA Above-water L (radiance)
 XGUV GUV Transfer Radiometer
 XPE XTRA Profiler E (irradiance)
 XPL XTRA Profiler L (radiance)
 XTRA Expandable Technologies for Radiometric Applications (XTRA)

SYMBOLS

0^+ The height immediately above the water surface.

E The irradiance.

$E_d(\lambda)$ The in-water spectral downward irradiance.

$E_d(0^+, \lambda)$ The above-water spectral global solar irradiance.

$E_i(\lambda)$ The above-water spectral indirect irradiance.

$E_s(\lambda)$ The above-water spectral global solar irradiance.

L The radiance.

$L_i(\lambda)$ The above-water spectral indirect (sky) radiance.

$L_T(\lambda)$ The above-water spectral total radiance from the sea surface.

$L_u(\lambda)$ The in-water spectral upwelling radiance.

$L_W(\lambda)$ The in-water spectral water-leaving radiance.

REFERENCES

- Bernhard, G., C.R. Booth, and J.C. Ehramjian, 2005: Real-time ultraviolet and column ozone from multichannel ultraviolet radiometers deployed in the National Science Foundation's ultraviolet monitoring network. *Opt. Eng.*, **44**, 041011-1–041011-12.
- Hooker, S.B., 2014: Mobilization Protocols for Hybrid Sensors for Environmental AOP Sampling (HySEAS) Observations. *NASA Tech. Pub. 2014-217518*, NASA Goddard Space Flight Center, Greenbelt, Maryland, 105 pp.
- , and J. Aiken, 1998: Calibration evaluation and radiometric testing of field radiometers with the SeaWiFS Quality Monitor (SQM). *J. Atmos. Oceanic Technol.*, **15**, 995–1,007.
- , G. Lazin, G. Zibordi, and S. McLean, 2002a: An evaluation of above- and in-water methods for determining water-leaving radiances. *J. Atmos. Oceanic Technol.*, **19**, 486–515.
- , S. McLean, J. Sherman, M. Small, G. Lazin, G. Zibordi, and J.W. Brown, 2002b: The Seventh SeaWiFS Inter-calibration Round-Robin Experiment (SIRREX-7), March 1999. *NASA Tech. Memo. 2002-206892*, Vol. 17, S.B. Hooker and E.R. Firestone, Eds., NASA Goddard Space Flight Center, Greenbelt, Maryland, 69 pp.
- , and G. Zibordi, 2005: Platform perturbations in above-water radiometry. *Appl. Opt.*, **44**, 553–567.
- , G. Bernhard, J.H. Morrow, C.R. Booth, T. Comer, R.N. Lind, and V. Quang, 2012: Optical Sensors for Planetary Radiant Energy (OSPRey): Calibration and Validation of Current and Next-Generation NASA Missions. *NASA Tech. Memo. 2012-215872*, NASA Goddard Space Flight Center, Greenbelt, Maryland, 117 pp.
- Johnson, B.C., P-S. Shaw, S.B. Hooker, and D. Lynch, 1998: Radiometric and engineering performance of the SeaWiFS Quality Monitor (SQM): A portable light source for field radiometers. *J. Atmos. Oceanic Technol.*, **15**, 1,008–1,022.
- Mueller, J.L., and R.W. Austin, 1992: Ocean Optics Protocols for SeaWiFS Validation. *NASA Tech. Memo. 104566*, Vol. 5, S.B. Hooker and E.R. Firestone, Eds., NASA Goddard Space Flight Center, Greenbelt, Maryland, 43 pp.
- Schmid, B., and C. Wehrli, 1995: Comparison of sun photometer calibration by use of the Langley technique and the standard lamp. *Appl. Opt.*, **34**, 4,500–4,512.
- , P.R. Spyak, S.F. Biggar, C. Wehrli, J. Sekler, T. In-gold, C. Mätzler, and N. Kämpfer, 1998: Evaluation of the applicability of solar and lamp radiometric calibrations of a precision sun photometer operating between 300 and 1,025 nm. *Appl. Opt.*, **18**, 3,923–3,941.
- World Meteorological Organization, 2003: WMO/GAW aerosol measurement procedures: Guidelines and recommendations. *Global Atmospheric Watch Rept., No. 153*, Geneva, Switzerland, 67 pp.

